International Ocean Discovery Program Expedition 369 Scientific Prospectus

Australia Cretaceous Climate and Tectonics

Tectonic, paleoclimate, and paleoceanographic history of the Mentelle Basin and Naturaliste Plateau at southern high latitudes during the Cretaceous

Richard Hobbs
Co-Chief Scientist
Department of Earth Sciences
Durham University
Durham DH1 3LE
United Kingdom

Brian Huber
Co-Chief Scientist
Department of Paleobiology, MRC-121
Smithsonian Institution
Washington DC 20013
USA

Kara A. Bogus
Expedition Project Manager/Staff Scientist
International Ocean Discovery Program
Texas A&M University
1000 Discovery Drive
College Station TX 77845
USA

IODP
INTERNATIONAL OCEAN DISCOVERY PROGRAM

Publisher's notes

This publication was prepared by the *JOIDES Resolution* Science Operator (JRSO) at Texas A&M University (TAMU) as an account of work performed under the International Ocean Discovery Program (IODP). Funding for IODP is provided by the following international partners:

National Science Foundation (NSF), United States
Ministry of Education, Culture, Sports, Science and Technology (MEXT), Japan
European Consortium for Ocean Research Drilling (ECORD)
Ministry of Science and Technology (MOST), People's Republic of China
Korea Institute of Geoscience and Mineral Resources (KIGAM)
Australia-New Zealand IODP Consortium (ANZIC)
Ministry of Earth Sciences (MoES), India
Coordination for Improvement of Higher Education Personnel (CAPES), Brazil

Portions of this work may have been published in whole or in part in other IODP documents or publications.

This IODP *Scientific Prospectus* is based on precruise *JOIDES Resolution* Facility advisory panel discussions and scientific input from the designated Co-Chief Scientists on behalf of the drilling proponents. During the course of the cruise, actual site operations may indicate to the Co-Chief Scientists, the Staff Scientist/Expedition Project Manager, and the Operations Superintendent that it would be scientifically or operationally advantageous to amend the plan detailed in this prospectus. It should be understood that any proposed changes to the science deliverables outlined in the plan presented here are contingent upon the approval of the IODP JRSO Director.

Disclaimer

Copyright

Citation

Hobbs, R., Huber, B., and Bogus, K.A., 2016. *Expedition 369 Scientific Prospectus: Australia Cretaceous Climate and Tectonics*. International Ocean Discovery Program. http://dx.doi.org/10.14379/iodp.sp.369.2016

ISSN
World Wide Web: 2332-1385

Abstract

The unique tectonic and paleoceanographic setting of the Naturaliste Plateau (NP) and Mentelle Basin (MB) offers an outstanding opportunity to investigate a range of scientific issues of global importance with particular relevance to climate change. Previous spot-core drilling at Deep Sea Drilling Project Site 258 in the western MB demonstrates the presence of an expanded upper Albian–lower Campanian chalk, marl, and claystone sequence that is nearly complete stratigraphically and yields calcareous microfossils that are mostly well preserved. This sediment package and the underlying Albian volcanic claystone unit extend across most of the MB and are targeted at the primary sites, located between 850 and 3900 m water depth. Coring the Cretaceous MB sequence at different paleodepths will allow recovery of material suitable for generating paleotemperature and biotic records that span the rise and collapse of the Cretaceous hothouse (including oceanic anoxic Events [OAEs] 1d and 2), providing insight to resultant changes in deep-water and surface water circulation that can be used to test predictions from earth system models. The high-paleolatitude (60°–62°S) location of the sites is especially important because of the enhanced sensitivity to changes in vertical gradients and surface water temperatures. Paleotemperature proxies and other data will reveal the timing, magnitude, and duration of peak hothouse temperatures and whether there were any cold snaps that would have allowed growth of a polar ice sheet. The sites are also well-positioned to monitor the mid-Eocene–early Oligocene opening of the Tasman Gateway and the Miocene–Pliocene restriction of the Indonesian Gateway; both passages have important effects on global oceanography and climate.

Comparison of the Cenomanian–Turonian OAE 2 interval that will be cored on the Great Australian Bight will establish whether significant changes in ocean circulation were coincident with OAE 2, and over what depth ranges, and whether OAE 2 in the high-latitude Southern Hemisphere was coincident with major changes in sea-surface temperature. Understanding the paleoceanographic changes in a regional context will provide a global test on models of Cenomanian–Turonian oceanographic and climatic evolution related both to extreme Turonian warmth and the evolution of OAE 2.

Drilling of Early Cretaceous volcanic rocks and underlying Jurassic(?) sediments in different parts of the MB will provide information on the timing of different stages of the Gondwana breakup and the nature of the various phases of volcanism, which will lead to an improved understanding of the evolution of the NP and MB.

Schedule for Expedition 369

International Ocean Discovery Program (IODP) Expedition 369 is based on IODP drilling proposal 760 Full2 and ancillary project letter (APL) 897 (available at **http://iodp.tamu.edu/scienceops/expeditions/australia_climate_tectonics.html**). Following ranking by the IODP Scientific Advisory Structure, the expedition was scheduled for the R/V *JOIDES Resolution*, operating under contract with the *JOIDES Resolution* Science Operator (JRSO). At the time of publication of this *Scientific Prospectus*, the expedition is scheduled to start in Hobart, Australia, on 26 September 2017 and end in Fremantle, Australia, on 26 November 2017. A total of 56 days will be available for the transit, drilling, coring, and downhole measurements described in this report (for the current detailed schedule, see **http://iodp.tamu.edu/scienceops**). Further details about the facilities aboard the *JOIDES Resolution* can be found at **http://iodp.tamu.edu/labs/ship.html**.

Introduction

Understanding the mechanisms, feedbacks, and temporal relationships that link climate dynamics between the polar regions and the tropics is of fundamental importance for reconstructing rapid climate change in the past, and hence to improve predictions for the future. High-resolution stratigraphic records from strategic locations around the globe, especially from the high-latitude ocean, are essential to achieve this broader goal. Within this context, past periods of extreme warmth, such as the Cretaceous hothouse and the Paleocene–Eocene Thermal Maximum, have attracted increasing research interest over recent years, providing often spectacular and sometimes contradictory insights into the mechanisms of natural, short-term change in climate, biogeochemical cycling, and ocean oxygenation. This expedition, primarily focusing on the Naturaliste Plateau (NP) and Mentelle Basin (MB), targets these fundamental objectives with specific goals of providing a high-latitude Southern Ocean site with expanded late Mesozoic and Cenozoic sections. The expedition will also vastly improve constraints on the tectonic history of the region.

Expedition 369 offers a unique opportunity to generate data about Southern Hemisphere, high-latitude Cretaceous climates—an aspect that is critically missing within the paleotemperature/paleoceanographic community—and to approximate cross-latitudinal thermal gradients with the tropics and equivalent latitudes in the Northern Hemisphere. Furthermore, it will allow us to obtain high-resolution stratigraphic records across the rise and collapse of the Cretaceous hothouse and understand potential correlation between the climate changes and tectonic history, especially major volcanic episodes in the region. These aspects are crucial to improve our understanding of climate and to inform the scientific modelling community on high-latitude Southern Hemisphere Cretaceous (and possibly older) records—a currently underexplored region.

Background and geological setting

Regional setting of the Naturaliste Plateau and Mentelle Basin

During the Jurassic break up of Gondwana, the NP was located near the junction of the Australian, Antarctic, and Greater India plates (Figure **F1**). The first stage of breakup occurred as India separated from Australia. This was followed much later, in the early Eocene, when Australia separated from Antarctica. The breakup on the southern margin took a long time and rifting is thought to have started in the Cenomanian–Turonian (Direen et al., 2011). Plate tectonic reconstructions corresponding to these early stages of rifting are poorly constrained and controversial (Williams et al., 2011; Gibbons et al., 2012, 2013; White et al., 2013).

The MB is part of a sequence of basins along the western margin of Australia (Powell et al., 1988; Gaina et al., 2003) and is separated from the Perth Basin by the basement high of the Leeuwin Block and the Yallingup shelf (Figure **F2**). The southern section of this margin is characterized by the distribution of onshore and offshore volcanic rocks, such as the Bunbury basalt (Frey et al., 1996; Coffin et al., 2002; Ingle et al., 2004; Gorter and Deighton, 2002); some authors have also considered it to be volcanic (e.g., Menzies et al., 2002). The Bunbury basalt contains two geochemical and age

groupings: the older "Casuarina type" is 132.2 ± 0.3 Ma (Hauterivian), and the younger "Gosselin type" is 123 Ma (Aptian) (Frey et al., 1996). The Gosselin type has been correlated with the Rajmahal traps of eastern India, which are dated at 118.1 ± 0.3 Ma and are thought to be linked to mantle plume activity associated with the formation of the Kerguelen Plateau (Kent et al., 1997, 2002; Coffin et al., 2002).

At around 95 Ma (Cenomanian), mafic volcanism marked the onset of rifting of the Broken Ridge microcontinent from the Kerguelen Plateau (Royer and Coffin, 1992; Tikku and Cande, 1998, 2000). Final break up between these features appears to have taken place at ~85 Ma. This ultimately resulted in the propagation of the Southeast Indian (mid-ocean) Ridge (e.g., Royer and Coffin, 1992; Gaina et al., 2003, 2007) toward the southeast.

Opening of the Australo-Antarctic Gulf

During the Cretaceous, the Great Australian Bight (GAB) was situated at the eastern tip of a partial seaway (the Australo-Antarctic Gulf [AAG]), with the NP in the open ocean at the western gateway that connected the AAG with the southern Indian Ocean. The AAG eventually widened to create the Southern Ocean by the mid-Cenozoic; the ~15 km thick post-Middle Jurassic sedimentary sequence that accumulated in the GAB contains the largest continental margin deltaic sequence deposited during the Late Cretaceous greenhouse. In 2007, Geoscience Australia recovered organic-rich (total organic carbon [TOC] up to 6.9%, hydrogen index [HI] ≤ 479 mg hydrocarbons/g TOC; Figure **F3**) marine black laminated shales of Cenomanian–Turonian age during dredging of an interpreted Albian–Santonian stratigraphic section exposed by canyon formation at the seaward edge of the Eyre Terrace in the western part of the GAB (Totterdell and Mitchell, 2009). The presence of mid-Cretaceous organic-rich marine sediments within this region had been predicted by an extensive seismic stratigraphic age model tied to nine petroleum exploration wells (Totterdell et al., 2008). The shales are of latest Cenomanian–earliest Turonian age, based on organic-walled dinoflagellate cyst assemblages composed of morphological variants of *Cribroperidinium edwardsii* and *Cyclonephelium compactum*, as well as *Eurydinium ingramii* and *Eurydinium saxoniense*. These constitute a typical association for oceanic anoxic Event (OAE) 2 in both hemispheres (Marshall and Batten, 1988). The molecular composition of the extractable organic matter displays a strong anoxic marine signature (e.g., high sulfur compound yields on pyrolysis), and the presence of age-diagnostic biomarkers (e.g., C_{26} 4-desmethylsterane) is consistent with a Cenomanian/Turonian (C/T) boundary age. A notable difference from other OAE 2 black shales, including those recovered at Deep Sea Drilling Project (DSDP) Site 258, is the lack of large enrichment in ^{13}C (Boreham, 2009); however, the ^{13}C analysis is limited by the noncontinuous nature of the dredged material. Despite the long-term subsea exposure of these samples, they have only been mildly impacted by oxidative weathering (Totterdell et al., 2008). Furthermore, vitrinite reflectance analysis confirms the immaturity of the shales (R_V max = 0.33%–0.5%).

Opening of the Tasman and Indonesian Gateways

The northward drift of Australia through the Cenozoic affected changes in two important ocean gateways: the opening of the Tasman Gateway between Australia and Antarctica in the middle Eocene–early Oligocene, and the restriction of the Indonesian Gateway between Australia and southeast Asia in the Miocene–Pliocene. Both passages have important effects on global oceanography and climate, and the NP/MB region is well situated to monitor their opening history and resultant effects on ocean circulation (Figure **F4**).

The Antarctic Circumpolar Current (ACC) in the Southern Ocean is central to the modern overturning circulation and surface heat redistribution (Toggweiler and Samuels, 1995, 1998; Wunsch, 2002; Sijp and England, 2004, 2005; Lumpkin and Speer, 2007). Although there is no significant restriction on the ACC in the modern Tasman Passage, the Tasman and Drake Passages both opened during the middle Eocene–Oligocene and the restriction to flow at the Tasman Passage would have been significant for ocean circulation, especially in the late Eocene–early Oligocene. During the Paleocene–Eocene, southern Australia would have been influenced more by subpolar (rather than the modern subtropical) gyres as a consequence of the closed or restricted Tasman Passage and more southerly position of Australia (e.g., Huber et al., 2004). During the early Eocene climatic optimum, however, temperatures in the southwest Pacific Ocean near Australia seem to have been warmer than climate models predict (Hollis et al., 2012). Cooling of the Antarctic margin relative to the Australian margin near Tasmania occurred early in the opening of the Tasman Passage, which was dated at 49–50 Ma according to the paleoceanographic interpretations of Bijl et al. (2013), and differentiation of deep water produced in the Southern Ocean relative to the North Atlantic began in the late middle Eocene (Cramer et al., 2009; Borrelli et al., 2014). However, plate tectonic reconstructions (Müller et al., 2000) indicate that separation of Australia and Antarctica near Tasmania occurred later (~43 Ma). Recovering material spanning this time interval thus provides an important opportunity to reconcile these tectonic and paleoceanographic interpretations.

The restricted surface flow through the Indonesian Gateway is essential to the surface heat flux in the Pacific and Indian Oceans and has been linked to El Niño Southern Oscillation (ENSO) dynamics and the global ocean overturning circulation (Gordon, 1986; Godfrey, 1996; Lee et al., 2002). The gradual restriction of the Indonesian Passage from deep-water throughflow in the late Oligocene–early Miocene to variable shallow flow in the Pliocene–Pleistocene is thought to have strongly affected surface heat distribution with potential links to the late Neogene cooling and Northern Hemisphere glaciation (Cane and Molnar, 2001; Kuhnt et al., 2004; Karas et al., 2009).

Cretaceous record from Site 258 (western Mentelle Basin)

During DSDP Leg 26, a 525 m sequence of marine sediments was discontinuously cored at Site 258 in the western MB (Davies, Luyendyk, et al., 1974); this spot coring achieved ~50% recovery, so in total only 22% of the possible core was recovered (Figure **F5**). During the mid-Cretaceous, this site was located at about 62°S (Figure **F1**). The upper 114 m was assigned to the upper Miocene–recent (a second hole, 258A, was drilled to 123.5 meters below seafloor [mbsf] with 59% recovery in this upper portion). The underlying 411 m was assigned to the mid- to Late Cretaceous, which consists of lower Albian detrital sandstone and glauconitic clay (Cores 26-258-25 through 26), lower–middle Albian ferruginous claystone, zeolite-bearing detrital clay, and coccolith-rich detrital clay (Cores 15–24), Cenomanian black shale (Cores 14–15), and Turonian–Campanian nannofossil chalk (Cores 5–13).

Foraminifers are abundant and show frosty preservation (presence of micrometer-scale overgrowths) in the chalk (Figure **F6A–F6B**) and are rare with glassy preservation (shells translucent with no infilling or overgrowths) in the Cenomanian and some Albian

clay-rich intervals (Figure F6C–F6D). Foraminifers are absent deeper than Core 26-258-20 and from some samples from Cores 16 and 17 (Herb, 1974). Marker species for standard low-latitude biostratigraphic schemes are often rare or absent at mid- to high latitudes, so correlation across latitudes requires developing and integrating separate higher latitude zonal schemes (Huber, 1992; Huber and Watkins, 1992; Petrizzo, 2000, 2001; Thibault et al., 2012). The paleomagnetic record spanning Chrons C29R through C33N at Maud Rise (Southern Ocean; Ocean Drilling Program [ODP] Site 690) and Southeast Georgia Rise (southern South Atlantic Ocean; ODP Site 700) enabled especially good middle Campanian–Maastrichtian age control for biostratigraphic correlation across the southern high latitudes (Huber, 1991).

Revised age interpretations are presented for the Cretaceous sequence at Site 258 using an updated austral chronostratigraphy (Figure F5). Significant revisions include the assignment of (1) Cores 26-258A-8 through 9 to the early Campanian (previously Santonian), (2) Cores 26-258-10 and 11 to the late Turonian (previously Coniacian), and (3) Core 26-258-14 to the late Cenomanian (previously Cenomanian undifferentiated). These biostratigraphic interpretations, in conjunction with seismic sequence interpretation (Figures F7, F8), demonstrate that there is a high probability of recovering a complete late Cenomanian through early Campanian sediment record, including the Cenomanian–Turonian OAE 2 interval, at the primary sites. Recovery of an expanded sequence of middle–upper Albian claystone yielding rare but well-preserved foraminifers and common to abundant and well-preserved calcareous nannofossils (Herb, 1974; Thierstein, 1974) suggests that recovery of late Albian OAE 1d is also very likely.

Seismic data

Seismic data acquired in 2004 and 2009 by Geoscience Australia (tied to Site 258) provide a regional survey to reappraise the stratigraphy, structural, and depositional history of the MB. These data have been interpreted by Maloney et al. (2011) and Borissova et al. (2010), and they largely agree on the stratigraphy of the MB to the Valanginian breakup unconformity. Maloney et al. (2011) do not provide a detailed interpretation below the extrusive (?) basalt layer that marks this boundary, whereas the interpretation of Borissova et al. (2010) is based on the wider stratigraphy from adjacent drilled basins on the Australian shelf and evidence from dredge samples around the margin of the plateau (Figure F9). Direct correlation between these pre-Valanginian units and those sampled in the more widely explored Perth Basin (Norvik, 2004) is not possible, as they are separated by the Yallingup shelf basement high (Figure F2).

The stratigraphy presented in Figures F7 and F8 is based on Borissova et al. (2010) (Figure F9). Relatively young Neogene carbonate oozes unconformably overlie Paleogene deep marine chalk. Occasional bright reflection events in this sequence are likely caused by thin chert bands, as shown at Site 258. This Paleogene chalk unconformably overlies Cretaceous coccolith-rich chalk that is underlain by Albian/Aptian claystones, which pinch out in the detrital sandstone and glauconitic clay. This sandstone/glauconitic clay sequence is floored by a high-amplitude reflection (not sampled at Site 258), interpreted to be caused by Valanginian volcanics. This horizon coincides with the onset of break up and separation of Greater India from Australia and a series of subsequent volcanic episodes related to the continuing break up on the northern and western margins of the NP. Prior rifting of the area is recorded by Early Cretaceous, Jurassic, and Permian/Triassic sequences, although the interpretation is somewhat speculative as it lacks well control. The affinity of the basement is not known, but dredge samples from around the plateau margins suggest a continental origin (Halpin et al., 2008).

Seismic studies/Site survey data

The supporting site survey data for Expedition 369 are archived in the IODP Site Survey Data Bank (**http://ssdb.iodp.org/SSDBquery/SSDBquery.php** [select Proposal Numbers P760 or P897]).

Scientific objectives

1. *Investigate the timing and causes for the rise and collapse of the Cretaceous hothouse and how this climate mode affected the climate-ocean system and oceanic biota.*

Compilations of deep-sea benthic foraminiferal and bulk carbonate $\delta^{18}O$ data reveal that the world ocean experienced long-term warming from the late Aptian through middle Cenomanian, maintained extremely warm temperatures from the late Cenomanian through Santonian with peak warmth during the Turonian (>20°C at mid-bathyal depths), and gradually returned to cooler values (~6°–8°C at mid-bathyal depths) during the Maastrichtian (Huber et al., 1995, 2002, 2011; Clarke and Jenkyns, 1999; Friedrich et al., 2012). New benthic and planktonic $\delta^{18}O$ values obtained from the Turonian at Site 258 support extreme high-latitude Turonian warmth (Figure F5). Still, these $\delta^{18}O$ values are problematically low and seem to defy straightforward explanations (Bice et al., 2003). These new analyses compared to existing stable isotope data (Huber et al., 1995, 2002) show large changes at times of known climatic shifts. Relative to low-latitude sites, high-latitude sites are both undersampled and respond more strongly to climate change.

Although the Cretaceous has long been characterized as too warm to sustain continental ice sheets (e.g., Barron, 1983; Frakes et al., 1992; Huber et al., 2002; Hay, 2008), coincidences between sea level variations (deduced from sequence stratigraphy) and $\delta^{18}O$ records have been proposed by some authors as evidence for the occasional existence of polar ice (e.g., Barrera et al., 1997; Miller et al., 1999, 2005; Stoll and Schrag, 2000; Gale et al., 2002; Bornemann et al., 2008) and winter sea ice (Bowman et al., 2012). The "greenhouse glaciers" hypothesis has been countered by evidence for diagenetic influence on bulk carbonate oxygen isotope records and stable tropical planktonic and benthic foraminiferal $\delta^{18}O$ data across several of the proposed cooling intervals (Huber et al., 2002; Moriya et al., 2007; Ando et al., 2009; MacLeod et al., 2013), Furthermore, TEX_{86} values from DSDP Site 511 suggest sea-surface temperatures (SSTs) during the Hauterivian–Aptian interval of 25°–30°C (Jenkyns et al., 2012).

High-resolution isotopic studies of samples from Expedition 369 sites should advance understanding and improve geographic documentation of major global climatic warming and cooling transitions during the Cretaceous. Recovery of more complete sections will lead to biostratigraphic refinements and improved regional to global correlations.

2. *Determine the relative roles of productivity, ocean temperature, and ocean circulation at high southern latitudes during Cretaceous oceanic anoxic events.*

OAEs are defined as short-lived (<1 My) episodes of enhanced deposition of organic carbon in a wide range of marine environments (Schlanger and Jenkyns, 1976) and are associated with prominent carbon isotope excursions in marine and terrestrial sequences

(Jenkyns, 1980, 2010; Arthur et al., 1988; Gröcke et al., 1999; Jahren et al., 2001; Ando et al., 2002; Jarvis et al., 2006). Generation of OAEs has been attributed to a rapid influx of volcanogenic and/or methanogenic CO_2 sources leading to abrupt temperature rise and an accelerated hydrological cycle, increased continental weathering and nutrient discharge to oceans and lakes, intensified upwelling, and an increase in organic productivity. Globally expressed Cretaceous OAEs occurred during the early Aptian (OAE 1a; ~120 Ma) and at the C/T boundary (OAE 2; ~94 Ma), whereas regionally recognized events occurred during the early Albian (OAE 1b; ~111 Ma) and late Albian (OAE 1d; ~100 Ma).

Cretaceous OAEs are best known from the Atlantic/Tethyan basins and surrounding continents, whereas Indian Ocean records are extremely limited. Evidence for euxinic waters in the region during OAE 2 is the presence of black shale with up to 6.9% TOC at multiple sites in the Bight Basin on the southern Australian margin (Totterdell et al., 2008). OAE deposits should be present at Site 258, Kerguelen (ODP Site 1138) and Exmouth Plateaus, and adjacent basinal areas (primarily ODP Site 763), but drilling strategies and poor recovery resulted in all cases of the cores missing the OAE record.

Recovery of a continuous record of the C/T boundary OAE 2 is anticipated at proposed Site WCED-4A on the GAB, northern MB proposed Site MBAS-8D, and western MB proposed Site MBAS-4B. At all three sites, the OAE 2 interval is at a shallow burial depth (260–400 mbsf), where sediments are thermally immature and biogenic preservation is expected to be good to excellent. It is likely that the late Albian OAE 1d will also be recovered at MB Sites MBAS-8D and MBAS-4B, where the projected burial depths are also relatively shallow. Observations and data will be compared among the GAB and MB sites and with other high-latitude OAE 2 sites to establish whether significant changes in ocean circulation were coincident with OAE 2, over what depth ranges (Zheng et al., 2013), and whether OAE 2 in the high-latitude Southern Hemisphere was coincident with major changes in SST (Jarvis et al., 2006). We are particularly interested in establishing whether the C/T succession in the GAB contains evidence for the "Plenus cold event," an important cooling (~4 to >5°C) event within OAE 2 known from the Northern Hemisphere. This event is associated with changes in surface water circulation (e.g., Zheng et al., 2013) and reoxygenation of bottom waters, but it remains unclear whether the Plenus cold event was a global or regional phenomenon. Data from the high southern latitudes are currently lacking (Jenkyns et al., 2012) and would address this critical gap in our model for OAE 2.

3. *Identify the main source regions for deep- and intermediate water masses in the southeast Indian Ocean and how these changed during Gondwana breakup.*

Over the past few years, study of Cretaceous intermediate and deep-water circulation patterns has been galvanized by an increase in published neodymium isotopic data (e.g., Jiménez Berrocoso et al., 2010; Robinson et al., 2010; MacLeod et al., 2011; Martin et al., 2012; Murphy and Thomas, 2012; Jung et al., 2013; Moiroud et al., 2013; Voigt et al., 2013; Zheng et al., 2013). Neodymium (Nd) isotopic values (expressed as ε_{Nd}) have emerged as a promising proxy for reconstructing past circulation, applicable across a wide range of depths including sub-carbonate compensation depth (CCD) carbonate-free abyssal samples.

Typically measured on either phosphatic fossils (fish teeth, bones, and scales) or oxides leached from bulk samples, ε_{Nd} values record a depositional to early diagenetic bottom water signature generally resistant to later diagenetic overprinting (Martin and Scher, 2004). The bottom water signature, in turn, reflects the ε_{Nd} value of that water mass' source region because Nd enters the ocean largely as riverine or eolian input, has a residence time shorter than the mixing time of the oceans, and has semiconservative behavior. Because ε_{Nd} values in likely source regions vary by 10–15 ε_{Nd} units compared to an analytical precision of ~0.3 units, stratigraphic trends in ε_{Nd} can be used to infer changes in circulation and mixing patterns through time. However, ε_{Nd} values of samples are also influenced by local to global volcanic inputs, and the bottom water ε_{Nd} signature of a water mass can be modified during circulation due to a high particle flux or boundary exchange, especially near detrital sources.

Cretaceous ε_{Nd} data have been used to test, refine, and revise earlier circulation hypotheses that were based largely on carbon and oxygen isotopes. They have also documented correlation between ε_{Nd} shifts and both long-term climate trends and shorter bioevents (e.g., OAE 2) and demonstrated a degree of complexity within and among sites not predicted by early studies. The latter is particularly true for the Southern Ocean where circulation changes, changes in water column stratification, volcanic inputs, and establishment of a widespread source of southern component water have all been invoked to explain observed patterns (e.g., Robinson and Vance, 2012; Murphy and Thomas, 2012; Jung et al., 2013; Voigt et al., 2013). Neodymium studies of samples from drill sites representing a range of depths within the MB/NP, when combined with parallel paleotemperature estimates from $\delta^{18}O$ and TEX_{86} and documentation of calcareous microfossil assemblages, should help reduce uncertainty in interpretation of previous studies.

4. *Characterize how oceanographic conditions changed at the Naturaliste Plateau during the Cenozoic opening of the Tasman Passage and restriction of the Indonesian Gateway.*

The MB drill sites are well positioned to monitor paleoceanographic variations in the Leeuwin Current/Undercurrent system. The surface Leeuwin Current (LC) is unique in flowing poleward along the eastern boundary of the Indian Ocean (Figure **F4**). It is caused by the north-south gradient between cooler waters to the south and warm surface waters along the northwestern Australian coast. These warmer waters are derived from the Indonesian Throughflow (ITF) that overrides the prevailing wind stress and results in the poleward flow (Pattiaratchi, 2006; Godfrey, 1996; Domingues et al., 2007; Waite et al., 2007). The strength of the LC varies seasonally with the ITF strength and interannually with ENSO dynamics, strengthening in winter and under La Niña conditions. The intermediate Leeuwin Undercurrent is derived from an eddy system associated with the Flinders Current near the NP (Middleton and Cirano, 2002; Waite et al., 2007; Meuleners et al., 2007; Divakaran and Brassington, 2011). The Flinders Current and Leeuwin Undercurrent are conduits of the Tasman leakage, a pathway for return flow to the North Atlantic Ocean of deep waters upwelled in the Pacific and a component of the Southern Hemisphere supergyre that links the subtropical gyres of the Atlantic, Pacific, and Indian Oceans (Speich et al., 2002, 2007; Ridgway and Dunn, 2007; van Sebille et al., 2012). The Tasman leakage allows interconnection of Antarctic Intermediate Water (AAIW) in the Pacific, Atlantic, and Indian Oceans, and the Flinders Current–Leeuwin Undercurrent system seems to play a role in the conversion of Subantarctic Mode Water to AAIW (Ridgway and Dunn, 2007). Deep water in the MB is derived from Antarctic Bottom Water (AABW) and lower Circumpolar Deep Water that enter the Perth Basin between the NP

and Broken Ridge, with substantial upwelling of AABW in the southern portion of the Perth Basin (Sloyan, 2006; McCartney and Donohue, 2007).

Drilling in the MB will complement previous drilling around Australia, especially off northwest and western Australia (DSDP Leg 27 and ODP Legs 122 and 123) and southern Australia and Tasmania (ODP Legs 182 and 189). Targeted sites will allow comparison of deep-water (Site MBAS-8D) and intermediate water (Site MBAS-9A) locations. Coring is expected to recover Paleocene–Eocene and upper Miocene–recent sequences. From regional seismic interpretations, these sequences should be mostly continuous as no regional unconformities have been identified. Expected recovered material will allow investigations of (1) the early Paleogene greenhouse climate at a high-latitude (~60°S) site, (2) oceanographic changes in the early stages of the opening of the Tasman Passage, and (3) oceanographic changes during the late stages of restriction of the Indonesian Passage.

5. *Resolve questions on the volcanic and sedimentary origins of the basin and provide vital stratigraphic control on the age and nature of the prebreakup succession.*

During the break up of Gondwana in the Early Cretaceous (Figure **F1**), the NP was located near the junction of three major plates: Australian, Antarctic, and Greater India. The breakup took place in two stages: first, India separated from Australia; then much later, in the early Eocene, Australia separated from Antarctica. The rifting of the southern margin was very slow, starting in the Cenomanian–Turonian (Direen et al., 2011), taking nearly 40 My before seafloor spreading was established. Plate tectonic reconstructions corresponding to these early stages of rifting are poorly constrained and controversial (Williams et al., 2011; Gibbons et al., 2012, 2013; White et al., 2013).

The interlinked aspects of the geology and evolution of the NP and MB suggest that recovering the volcanic rocks at the Valanginian/late Hauterivian unconformity will further our understanding of this region. Drilling the unconformity at Sites MBAS-8D and MBAS-4B will provide information on the timing and position of the breakup (both on the western and southern margin, using paleomagnetic studies and $^{40}Ar/^{39}Ar$ dating of lavas), on the nature of the various phases of volcanism (core description, petrophysics, and geochemical and isotopic study), on geographic and environmental reconstructions, and on the depositional history of the basin.

The principal cause of high-amplitude discontinuous reflectors overlying the Valanginian breakup unconformity corresponds to extrusive volcanics that flowed into the MB at the time of the breakup. Dredging on the steep flanks of the NP recovered a suite of metamorphic (Halpin et al., 2008) and volcanic rocks (Crawford et al., 2006), indicating that the plateau is underpinned by continental basement overlain by volcanic rocks. Interestingly, to the south in the Diamantina Zone, both metamorphic and mantle rocks were recovered (Beslier et al., 2004), suggesting extreme thinning of the continental crust.

Drilling into the Valanginian volcanics and pre-Valanginian sediments (Sites MBAS-8D, MBAS-4B, and MBAS-9A) will provide vital stratigraphic control on the age and nature of the prebreakup succession, and recovery of pre-Valanginian basalts will address questions on the origins and age of the volcanics. The results from this expedition will address a number of key tectonics questions for the region.

Drilling and coring strategy

Previous work by both academia and industry has provided abundant site survey data and limited physical material (e.g., Site 258, dredge samples adjacent to proposed Site WCED-4A; Totterdell and Mitchell, 2009). Using these data, we identified four primary sites (WCED-4A, MBAS-8D, MBAS-4B, and MBAS-9A) and five alternate sites (MBAS-8B, MBAS-4C, MBAS-6A, MBAS-3C, and MBAS-5B) (Figure **F2**) that will achieve the stated expedition science objectives.

Our primary drilling and coring strategy is summarized in Table **T1**. Our coring strategy at Site WCED-4A in the GAB consists of a single rotary core barrel (RCB) hole to total depth (570 mbsf). This strategy is designed to maximize the chances of recovering the material of interest (Cenomanian–Turonian black shales and OAE 2) within a reasonable operational time window. From Site WCED-4A, we will proceed to Site MBAS-8D in the MB, where the planned operations include using the advanced piston corer (APC) in two holes to ~300 mbsf or APC refusal. APC refusal is an estimated depth that is formation dependent. It is usually defined two ways: (1) a complete stroke (determined by standpipe pressure) is not achieved because of formation hardness or (2) excessive force (>100,000 lb) is required to pull the core barrel out of the formation because it is too cohesive. In cases where a full stroke with the full-length (9.5 m) APC is not achieved, the half-length APC (HLAPC, 4.8 m core barrel) technique may be used to deepen APC refusal. The decision to use the HLAPC will be strongly influenced by operational timing. In the second APC hole, the total penetration depth will be increased beyond APC refusal using the extended core barrel (XCB) technique. A third hole is planned to reach the target depth (1100 mbsf) at Site MBAS-8D using the RCB system. This deep penetration is necessary to allow us to core the underlying basalt sequence at the Valanginian unconformity, a key objective of this expedition.

Following operations at Site MBAS-8D, the next planned site (MBAS-4B; adjacent to Site 258) will consist of two APC/XCB holes to 730 and 490 mbsf. These holes are targeted to recover duplicates of any OAEs and penetrate into to the basalt sequence. Operations at the final primary site (MBAS-9A) consist of two APC/XCB holes to 364 mbsf along with one RCB hole to 1200 mbsf and will sample the pre-Valanginian sedimentary succession. Together, the sites will address Cenozoic changes in the Tasman and Indonesian Gateways.

All planned APC, HLAPC, and RCB coring will use nonmagnetic core barrels as much as possible. Following coring operations in the deepest holes of each site, the holes will be conditioned, displaced with logging mud, and logged (see **Downhole measurements strategy**).

Downhole measurements strategy

Formation temperature measurements

While APC coring in the first hole at each site, a series of formation temperature measurements using the advanced piston corer temperature tool (APCT-3) are planned.

Core orientation

All APC cores will be oriented with the Icefield MI-5 orientation tool and will use nonmagnetic core barrels as much as possible.

Downhole wireline logging

Wireline logging is currently planned for the deepest hole at each of our primary sites, but implementation will actually depend on hole conditions. The wireline logging plan aims to provide information on in situ formation properties (lithologies, structures, and petrophysics) and allow for core-log-seismic integration.

Three standard IODP tool string configurations will be deployed: the triple combination (triple combo), Formation MicroScanner (FMS)-sonic, and Versatile Seismic Imager (VSI).

At each site, the first tool string deployed will be the triple combo, which measures density, neutron porosity, resistivity, and natural gamma radiation (NGR) and spectral gamma ray, along with borehole diameter via calipers. The caliper log provided by the density tool will allow an assessment of hole conditions and the potential for success of subsequent logging runs. The FMS-sonic tool string is the second logging run planned and will record gamma ray, sonic velocity (for compressional and shear waves), and high-resolution electrical images. The compressional velocity logs will be combined with the density logs to generate synthetic seismograms for detailed seismic-log correlations. To calibrate the integration of log and seismic data, the third run in each hole will be a vertical seismic profile (VSP) recorded with the VSI, which requires the use of a seismic sound source. The expected spacing between stations is 25 m over the entire open interval of each hole logged. Spacing could be adjusted for specific targets or hole conditions. The seismic sound source used during the check shot/VSP survey will be subject to the IODP marine mammal policy, including daylight-only operation of the sound source, and may have to be postponed or canceled if certain policy conditions are not met. For more information on specific logging tools, please refer to **http://iodp.tamu.edu/tools/logging**.

Downhole measurements will be the only data available where core recovery is incomplete. Moreover, the data will provide common measurements for core-log integration (density, NGR, and magnetic susceptibility) and establish the link between borehole and core features and reflectors on seismic profiles by synthetic seismograms and VSP.

Risks and contingency

There are several risks to achieving the objectives of this expedition. Sea state and the resulting heave behavior of the ship as a result of weather conditions are critical. Additionally, the nature of the sediments and basalts could negatively impact coring/logging operations, hole stability, core recovery and quality, and rate of penetration. Finally, this is an ambitious coring plan and site prioritization is essential to balance the diverse scientific objectives. This has been managed, in part, by the order in which we plan to core the sites as well as the time allocated to each site. For example, coring at Site MBAS-8D is expected to penetrate into and recover the basalt sequence. As such, coring to the total depth approved by the Environmental Protection and Safety Panel at Site MBAS-4B (880 mbsf), the next site in the operations sequence, may not be undertaken if time becomes restricted, as the same basalts are expected there. However, if operations at Site MBAS-8D do not allow us to recover the basalts, we will deepen our planned operations at Site MBAS-4B to 880 mbsf. Finally, a series of alternate sites are available for contingency operations (Table **T2**).

Sampling and data sharing strategy

Shipboard and shore-based researchers should refer to the IODP Sample, Data, and Obligations Policy and Implementation Guidelines at **http://www.iodp.org/policies-and-guidelines**. This document outlines the policy for distributing IODP samples and data to research scientists, curators, and educators. The document also defines the obligations that sample and data recipients incur. The Sample Allocation Committee (SAC) (composed of Co-Chief Scientists, Staff Scientist, and IODP Curator on shore and curatorial representative on board the ship) will work with the entire scientific party to formulate a formal expedition-specific sampling plan for shipboard and postcruise sampling.

Shipboard scientists are expected to submit postcruise research plans, including sample/data requests (at **http://web.iodp.tamu.edu/sdrm**) no later than 3 months before the beginning of the expedition. This timing is necessary to coordinate the research to be conducted and to ensure that the scientific objectives are achieved. Based on the requests (shore based and shipboard) submitted by this deadline, the SAC will prepare a tentative sampling and data plan. This plan will be subject to modification depending upon actual core recovery and collaborations that may evolve between scientists during the expedition. The SAC must approve any modifications to this strategy during the expedition.

All personal sample frequencies and sizes must be justified on a scientific basis and will depend on core recovery, the full spectrum of other sample requests, and the expedition objectives. Some redundancy of measurements is unavoidable, but minimizing the duplication of measurements among the shipboard party and identified shore-based collaborators will be a factor in evaluating sample/data requests. All shipboard scientists and approved shore-based requesters are expected to collaborate and cooperate within the framework of this plan. Sampling for individual scientist's postcruise research will completely depend on core recovery and may either take place on the ship or be deferred until after the cruise. Currently, we anticipate ~3.4 km of recovered material along with several intervals of high scientific interest (i.e., OAEs). Thus, the decision regarding personal sampling on board versus a postcruise sampling party will be made during the expedition when core recovery and quality are better known.

If a postcruise sampling party is deemed necessary, the cores will be delivered to the Gulf Coast Repository (College Station, TX) until sampling, after which they will be sent to the Kochi Core Center (KCC) (Kochi, Japan). If a sampling party is not required, the cores will be delivered directly to the KCC after the expedition. All collected data and samples will be protected by a 1 y moratorium during which time they are available only to the Expedition 369 science party and approved shore-based participants. This moratorium will extend 1 y following either the end of the expedition or the completion of a postcruise sampling party.

Expedition scientists and scientific participants

The current list of participants for Expedition 369 can be found at: **http://iodp.tamu.edu/scienceops/expeditions/australia_climate_tectonics.html**.

References

Ando, A., Huber, B.T., MacLeod, K.G., Ohta, T., and Khim, B.-K., 009. Blake Nose stable isotopic evidence against the mid-Cenomanian glaciation hypothesis. *Geology*, 37(5):451–454. **http://dx.doi.org/10.1130/G25580A.1**

Ando, A., Kakegawa, T., Takashima, R., and Saito, T., 2002. New perspective on Aptian carbon isotope stratigraphy: data from $\delta^{13}C$ records of terrestrial organic matter. *Geology*, 30(3):227–230. **http://dx.doi.org/10.1130/0091-7613(2002)030<0227:NPOACI>2.0.CO;2**

Arthur, M.A., Dean, W.E., and Pratt, L.M., 1988. Geochemical and climatic effects of increased marine organic carbon burial at the Cenomanian/Turonian boundary. *Nature,* 335(6192):714–717. **http://dx.doi.org/10.1038/335714a0**

Barrera, E., Savin, S.M., Thomas, E., and Jones, C.E., 1997. Evidence for thermohaline-circulation reversals controlled by sea- level change in the latest Cretaceous. *Geology,* 25(8):715–718. **http://dx.doi.org/10.1130/0091-7613(1997)025<0715:EFTCRC>2.3.CO;2**

Barron, E.J., 1983. A warm, equable Cretaceous: the nature of the problem. *Earth-Science Reviews,* 19(4):305–338. **http://dx.doi.org/10.1016/0012-8252(83)90001-6**

Beslier, M.-O., Royer, J.-Y., Girardeau, J., Hill, P.J., Boeuf, E., Buchanan, C., Chatin, F., Jacovetti, G., Moreau, A., Munschy, M., Partouche, C., Robert, U., and Thomas, S., 2004. A wide ocean-continent transition along the south-west Australian margin: first results of the MARGAU/MD110 cruise. *Bulletin de la Société Géologique de France,* 175(6):629–641. **http://dx.doi.org/10.2113/175.6.629**

Bice, K.L., Huber, B.T., and Norris, R.D., 2003. Extreme polar warmth during the Cretaceous greenhouse? Paradox of the late Turonian $\delta^{18}O$ record at Deep Sea Drilling Project Site 511. *Paleoceanography,* 18(2):1031. **http://dx.doi.org/10.1029/2002PA000848**

Bijl, P.K., Bendle, J.A.P., Bohaty, S.M., Pross, J., Schouten, S., Tauxe, L., Stickley, C.E., McKay, R.M., Röhl, U., Olney, M., Sluijs, A., Escutia, C., Brinkhuis, H., and Expedition 318 Scientists, 2013. Eocene cooling linked to early flow across the Tasmanian Gateway. *Proceedings of the National Academy of Sciences of the United States of America,* 110(24):9645–9650. **http://dx.doi.org/10.1073/pnas.1220872110**

Boreham, C., 009. Organic geochemistry—source rock characterisation. *In* Totterdell, J., and Mitchell, C. (Eds.), *Bight Basin Geological Sampling and Seepage Survey: R/V* Southern Surveyor *Survey SS01/2007.* Geoscience Australia, 2009/24:36–60. **http://www.ga.gov.au/metadata-gateway/metadata/record/68689/**

Borissova, I., 2002. *Geological Framework of the Naturaliste Plateau.* Geoscience Australia, 2002/20. **http://www.ga.gov.au/metadata-gateway/metadata/record/40535/**

Borissova, I., Bradshaw, B.E., Nicholson, C., Struckmeyer, H.I.M., and Payne, D., 2010. New exploration opportunities on the southwest Australian margin: deep-water frontier Mentelle Basin. *APPEA Journal,* 50:1–13.

Bornemann, A., Norris, R.D., Friedrich, O., Beckmann, B., Schouten, S., Sinninghe Damsté, J.S., Vogel, J., Hofmann, P., and Wagner, T., 2008. Isotopic evidence for glaciation during the Cretaceous supergreenhouse. *Science,* 319(5860):189–192. **http://dx.doi.org/10.1126/science.1148777**

Borrelli, C., Cramer, B.S., and Katz, M.E., 2014. Bipolar Atlantic deepwater circulation in the middle-late Eocene: effects of Southern Ocean gateway openings. *Paleoceanography,* 29(4):308–327. **http://dx.doi.org/10.1002/2012PA002444**

Bowman, V.C., Francis, J.E., Riding, J.B., Hunter, S.J., and Haywood, A.M., 2012. A latest Cretaceous to earliest Paleogene dinoflagellate cyst zonation from Antarctica, and implications for phytoprovincialism in the high southern latitudes. *Review of Palaeobotany and Palynology,* 171:40–56. **http://dx.doi.org/10.1016/j.revpalbo.2011.11.004**

Cane, M.A., and Molnar, P., 2001. Closing of the Indonesian Seaway as a precursor to East African aridification around 3–4 million years ago. *Nature,* 411(6834):157–162. **http://dx.doi.org/10.1038/35075500**

Clarke, L.J., and Jenkyns, H.C., 1999. New oxygen isotope evidence for long-term Cretaceous climatic change in the Southern Hemisphere. *Geology,* 27(8):699–702. **http://dx.doi.org/10.1130/0091-7613(1999)027<0699:NOIEFL>2.3.CO;2**

Coffin, M.F., Pringle, M.S., Duncan, R.A., Gladczenko, T.P., Storey, M., Müller, R.D., and Gahagan, L.A., 2002. Kerguelen hotspot magma output since 130 Ma. *Journal of Petrology,* 43(7):1121–1137. **http://dx.doi.org/10.1093/petrology/43.7.1121**

Cramer, B.S., Toggweiler, J.R., Wright, J.D., Katz, M.E., and Miller, K.G., 2009. Ocean overturning since the Late Cretaceous: inferences from a new benthic foraminiferal isotope compilation. *Paleoceanography,* 24(4). **http://dx.doi.org/10.1029/2008PA001683**

Crawford, A.J., Direen, N.G., Coffin, M.F., Cohen, B., Paul, B., and Mitrovic, L., 2006. Extensive basaltic magmatism on the Naturaliste Plateau, offshore SW Australia. *Geochimica et Cosmochimica Acta,* 70(18):A116. **http://dx.doi.org/10.1016/j.gca.2006.06.145**

Davies, T.A., Luyendyk, B.P., et al., 1974. *Initial Reports of the Deep Sea Drilling Project,* 26: Washington, DC (U.S. Government Printing Office). **http://dx.doi.org/10.2973/dsdp.proc.26.1974**

Direen, N.G., Stagg, H.M.J., Symonds, P.A., and Colwell, J.B., 2011. Dominant symmetry of a conjugate southern Australian and East Antarctic magma-poor rifted margin segment. *Geochemistry, Geophysics, Geosystems,* 12(2):Q02006. **http://dx.doi.org/10.1029/2010GC003306**

Divakaran, P., and Brassington, G.B., 2011. Arterial ocean circulation of the southeast Indian Ocean. *Geophysical Research Letters,* 38(1):L01802. **http://dx.doi.org/10.1029/2010GL045574**

Domingues, C.M., Maltrud, M.E., Wijffels, S.E., Church, J.A., and Tomczak, M., 2007. Simulated Lagrangian pathways between the Leeuwin Current System and the upper-ocean circulation of the southeast Indian Ocean. *Deep Sea Research Part II: Topical Studies in Oceanography,* 54(8–10):797–817. **http://dx.doi.org/10.1016/j.dsr2.2006.10.003**

Frakes, L.A., Francis, J.E., and Syktus, J.I., 1992. *Climate Modes of the Phanerozoic:* Cambridge, United Kingdom (Cambridge University Press).

Frey, F.A., McNaughton, N.J., Nelson, D.R., deLaeter, J.R., and Duncan, R.A., 1996. Petrogenesis of the Bunbury Basalt, Western Australia: interaction between the Kerguelen plume and Gondwana lithosphere? *Earth and Planetary Science Letters,* 144(1–2):163–183. **http://dx.doi.org/10.1016/0012-821X(96)00150-1**

Friedrich, O., Schiebel, R., Wilson, P.A., Weldeab, S., Beer, C.J., Cooper, M.J., and Fiebig, J., 2012. Influence of test size, water depth, and ecology on Mg/Ca, Sr/Ca, $\delta^{18}O$ and $\delta^{13}C$ in nine modern species of planktic foraminifers. *Earth and Planetary Science Letters,* 319–320:133–145. **http://dx.doi.org/10.1016/j.epsl.2011.12.002**

Gaina, C., Müller, R.D., Brown, B.J., and Ishihara, T., 2003. Microcontinent formation around Australia. *In* Hillis, R., and Müller, R.D. (Eds.), *The Evolution and Dynamics of the Australian Plate.* Special Paper - Geology Society of America, 372:405–416. **http://dx.doi.org/10.1130/0-8137-2372-8.405**

Gaina, C., Müller, R.D., Brown, B., Ishihara, T., and Ivanov, S., 2007. Breakup and early seafloor spreading between India and Antarctica. *Geophysical Journal International,* 170(1):151–169. **http://dx.doi.org/10.1111/j.1365-246X.2007.03450.x**

Gale, A.S., Hardenbol, J., Hathway, B., Kennedy, W.J., Young, J.R., and Phansalkar, V., 2002. Global correlation of Cenomanian (Upper Cretaceous) sequences: evidence for Milankovitch control on sea level. *Geology,* 30(4):291–294. **http://dx.doi.org/10.1130/0091-7613(2002)030<0291:GCOCUC>2.0.CO;2**

Gibbons, A.D., Barckhausen, U., van den Bogaard, P., Hoernle, K., Werner, R., Whittaker, J.M., and Müller, R.D., 2012. Constraining the Jurassic extent of Greater India: tectonic evolution of the West Australian margin. *Geochemistry, Geophysics, Geosystems,* 13:Q05W13. **http://dx.doi.org/10.1029/2011GC003919**

Gibbons, A.D., Whittaker, J.M., and Müller, R.D., 2013. The breakup of East Gondwana: assimilating constraints from Cretaceous ocean basins around India into a best-fit tectonic model. *Journal of Geophysical Research: Solid Earth,* 118(3):808–822. **http://dx.doi.org/10.1002/jgrb.50079**

Godfrey, J.S., 1996. The effect of the Indonesian throughflow on ocean circulation and heat exchange with the atmosphere: a review. *Journal of Geo-*

physical Research: Oceans, 101(C5):12217–12237. **http://dx.doi.org/10.1029/95JC03860**

Gordon, A.L., 1986. Interocean exchange of thermocline water. *Journal of Geophysical Research: Oceans,* 91(C4):5037–5046. **http://dx.doi.org/10.1029/JC091iC04p05037**

Gorter, J.D., and Deighton, I., 2002. Effects of igneous activity in the offshore northern Perth Basin—evidence from petroleum exploration wells, 2D seismic and magnetic surveys. *In* Keep, M., and Moss, S.J. (Eds.), *The Sedimentary Basins of Western Australia.* Proceedings of the Petroleum Exploration Society of Australia Symposium, 3:875–899. **https://www.pesa.com.au/library/the_sedimentary_basins_of_wa_3_p875-899-pdf**

Gröcke, D.R., Hesselbo, S.P., and Jenkyns, H.C., 1999. Carbon-isotope composition of Lower Cretaceous fossil wood: ocean-atmosphere chemistry and relation to sea-level change. *Geology,* 27(2):155–158. **http://dx.doi.org/10.1130/0091-7613(1999)027<0155:CICOLC>2.3.CO;2**

Halpin, J.A., Crawford, A.J., Direen, N.G., Coffin, M.F., Forbes, C.J., and Borissova, I., 2008. Naturaliste Plateau, offshore Western Australia: a submarine window into Gondwana assembly and breakup. *Geology,* 36(10):807–810. **http://dx.doi.org/10.1130/G25059A.1**

Hay, W.W., 2008. Evolving ideas about the Cretaceous climate and ocean circulation. *Cretaceous Research,* 29(5–6):725–753. **http://dx.doi.org/10.1016/j.cretres.2008.05.025**

Hay, W.W., DeConto, R.M., Wold, C.N., Wilson, K.M., Voigt, S., Schulz, M., Rossby Wold, A., Dullo, W.-C., Ronov, A.B., Balukhovsky, A.N., and Söding, E., 1999. Alternative global Cretaceous paleogeography. *In* Barrera, E., and Johnson, C.C. (Eds.), *Evolution of the Cretaceous Ocean-Climate System*. Special Paper - Geological Society of America, 332:1–47. **http://dx.doi.org/10.1130/0-8137-2332-9.1**

Herb, R., 1974. Cretaceous planktonic foraminifera from the eastern Indian Ocean. *In* Davies, T.A., Luyendyk, B.P., et al., *Initial Reports of the Deep Sea Drilling Project,* 26: Washington, DC (U.S. Government Printing Office), 745–770. **http://dx.doi.org/10.2973/dsdp.proc.26.132.1974**

Hollis, C.J., Taylor, K.W.R., Handley, L., Pancost, R.D., Huber, M., Creech, J.B., Hines, B.R., Crouch, E.M., Morgans, H.E.G., Crampton, J.S., Gibbs, S., Pearson, P.N., and Zachos, J.C., 2012. Early Paleogene temperature history of the Southwest Pacific Ocean: reconciling proxies and models. *Earth and Planetary Science Letters,* 349–350:53–66. **http://dx.doi.org/10.1016/j.epsl.2012.06.024**

Huber, B.T., 1991. Maestrichtian planktonic foraminifer biostratigraphy and the Cretaceous/Tertiary boundary at Hole 738C (Kerguelen Plateau, southern Indian Ocean). *In* Barron, J., Larsen, B., et al., *Proceedings of the Ocean Drilling Program, Scientific Results,* 119: College Station, TX (Ocean Drilling Program), 451–465. **http://dx.doi.org/10.2973/odp.proc.sr.119.143.1991**

Huber, B.T., 1992. Paleobiogeography of Campanian–Maastrichtian foraminifera in the southern high latitudes. *Palaeogeography, Palaeoclimatology, Palaeoecology,* 92(3–4):325–360. **http://dx.doi.org/10.1016/0031-0182(92)90090-R**

Huber, B.T., Hodell, D.A., and Hamilton, C.P., 1995. Mid- to Late Cretaceous climate of the southern high latitudes: stable isotopic evidence for minimal equator-to-pole thermal gradients. *Geological Society of America Bulletin,* 107(10):1164–1191. **http://dx.doi.org/10.1130/0016-7606(1995)107<1164:MLCCOT>2.3.CO;2**

Huber, B.T., MacLeod, K.G., Gröcke, D.R., and Kucera, M., 2011. Paleotemperature and paleosalinity inferences and chemostratigraphy across the Aptian/Albian boundary in the subtropical North Atlantic. *Paleoceanography,* 26(4). **http://dx.doi.org/10.1029/2011PA002178**

Huber, B.T., Norris, R.D., and MacLeod, K.G., 2002. Deep sea paleotemperature record of extreme warmth during the Cretaceous. *Geology,* 30(2):123–126. **http://dx.doi.org/10.1130/0091-7613(2002)030<0123:DSPROE>2.0.CO;2**

Huber, B.T., and Watkins, D.K., 1992. Biogeography of Campanian-Maastrichtian calcareous plankton in the region of the Southern Ocean: paleogeographic and paleoclimatic implications. *In* Kennett, J.P., and Warnke, D.A. (Eds.), *The Antarctic Paleoenvironment: A Perspective on Global Change.* Antarctic Research Series, 56:31–60.

Huber, M., Brinkhuis, H., Stickley, C.E., Döös, K., Sluijs, A., Warnaar, J., Schellenberg, S.A., and Williams, G.L., 2004. Eocene circulation of the Southern Ocean: was Antarctica kept warm by subtropical waters? *Paleoceanography,* 19(4):PA4026. **http://dx.doi.org/10.1029/2004PA001014**

Ingle, S., Scoates, J.S., Weis, D., Brügmann, G., and Kent, R.W., 2004. Origin of Cretaceous continental tholeiites in southwestern Australia and eastern India: insights from Hf and Os isotopes. *Chemical Geology,* 209(1–2):83–106. **http://dx.doi.org/10.1016/j.chemgeo.2004.04.023**

Jahren, A.H., Arens, N.C., Sarmiento, G., Guerrero, J., and Amundson, R., 2001. Terrestrial record of methane hydrate dissociation in the Early Cretaceous. *Geology,* 29(2):159–162. **http://dx.doi.org/10.1130/0091-7613(2001)029<0159:TROMHD>2.0.CO;2**

Jarvis, I., Gale, A.S., Jenkyns, H.C., and Pearce, M.A., 2006. Secular variation in Late Cretaceous carbon isotopes: a new $\delta^{13}C$ carbonate reference curve for the Cenomanian–Campanian (99.6–70.6 Ma). *Geological Magazine,* 143(5):561–608. **http://dx.doi.org/10.1017/S0016756806002421**

Jenkyns, H.C., 1980. Cretaceous anoxic events: from continents to oceans. *Journal of the Geological Society,* 137(2):171–188. **http://dx.doi.org/10.1144/gsjgs.137.2.0171**

Jenkyns, H.C., 2010. Geochemistry of oceanic anoxic events. *Geochemistry, Geophysics, Geosystems,* 11(3):Q03004. **http://dx.doi.org/10.1029/2009GC002788**

Jenkyns, H.C., Schouten-Huibers, L., Schouten, S., and Sinninghe Damsté, J.S., 2012. Warm Middle Jurassic–Early Cretaceous high-latitude sea-surface temperatures from the Southern Ocean. *Climate of the Past,* 8(1):215–226. **http://dx.doi.org/10.5194/cp-8-215-2012**

Jiménez Berrocoso, Á., MacLeod, K.G., Huber, B.T., Lees, J.A., Wendler, I., Bown, P.R., Mweneinda, A.K., Isaza Londoño, C., and Singano, J.M., 2010. Lithostratigraphy, biostratigraphy and chemostratigraphy of Upper Cretaceous sediments from southern Tanzania: Tanzania Drilling Project Sites 21–26. *Journal of African Earth Sciences,* 57(1–2):47–69. **http://dx.doi.org/10.1016/j.jafrearsci.2009.07.010**

Jung, C., Voigt, S., Friedrich, O., Koch, M.C., and Frank, M., 2013. Campanian–Maastrichtian ocean circulation in the tropical Pacific. *Paleoceanography,* 28(3):562–573. **http://dx.doi.org/10.1002/palo.20051**

Karas, C., Nürnberg, D., Gupta, A.K., Tiedemann, R., Mohan, K., and Bickert, T., 2009. Mid-Pliocene climate change amplified by a switch in Indonesian subsurface throughflow. *Nature Geoscience,* 2(6):434–438. **http://dx.doi.org/10.1038/ngeo520**

Kent, R.W., Pringle, M.S., Müller, R.D., Saunders, A.D., and Ghose, N.C., 2002. $^{40}Ar/^{39}Ar$ geochronology of the Rajmahal basalts, India, and their relationship to the Kerguelen Plateau. *Journal of Petrology,* 43(7):1141–1154. **http://dx.doi.org/10.1093/petrology/43.7.1141**

Kent, W., Saunders, A.D., Kempton, P.D., and Ghose, N.C., 1997. Rajmahal basalts, eastern India: mantle sources and melt distribution at a volcanic rifted margin. *In* Mahoney, J.J., and Coffin, M.F. (Eds.), *Large Igneous Provinces: Continental, Oceanic and Planetary Flood Volcanism.* Geophysical Monograph, 100:145–182.

Kuhnt, W., Holbourn, A., Hall, R., Zuvela, M., and Käse, R., 2004. Neogene history of the Indonesian Throughflow. *In* Clift, P., Wang, P., Kuhnt, W., and Hayes, D. (Eds.), *Continent-Ocean Interactions within East Asian Marginal Seas.* Geophysical Monograph, 149:299–320. **http://dx.doi.org/10.1029/149GM16**

Lee, T., Fukumori, I., Menemenlis, D., Xing, Z., and Fu, L.-L., 2002. Effects of the Indonesian throughflow on the Pacific and Indian Oceans. *Journal of Physical Oceanography,* 32(5):1404–1429. **http://dx.doi.org/10.1175/1520-0485(2002)032<1404:EOTITO>2.0.CO;2**

Lumpkin, R., and Speer, K., 2007. Global ocean meridional overturning. *Journal of Physical Oceanography,* 37(10):2550–2562. **http://dx.doi.org/10.1175/JPO3130.1**

MacLeod, K.G., Huber, B.T., Jiménez Berrocoso, Á., and Wendler, I., 2013. A stable and hot Turonian without glacial $\delta^{18}O$ excursions is indicated by

exquisitely preserved Tanzanian foraminifera. *Geology,* 41(10):1083–1086. **http://dx.doi.org/10.1130/G34510.1**

MacLeod, K.G., Londoño, C.I., Martin, E.E., Jiménez Berrocoso, Á., and Basak, C., 2011. Changes in North Atlantic circulation at the end of the Cretaceous greenhouse interval. *Nature Geoscience,* 4(11):779–782. **http://dx.doi.org/10.1038/ngeo1284**

Maloney, D., Sargent, C., Direen, N.G., Hobbs, R.W., and Gröcke, D.R., 2011. Re-evaluation of the Mentelle Basin, a polyphase rifted margin basin, offshore southwest Australia: new insights from integrated regional seismic datasets. *Solid Earth,* 2(2):107–123. **http://dx.doi.org/10.5194/se-2-107-2011**

Marshall, K.L., and Batten, D.J., 1988. Dinoflagellate cyst associations in Cenomanian–Turonian "black shale" sequences of northern Europe. *Review of Palaeobotany and Palynology,* 54(1–2):85–103. **http://dx.doi.org/10.1016/0034-6667(88)90006-1**

Martin, E.E., MacLeod, K.G., Jiménez Berrocoso, A., and Bourbon, E., 2012. Water mass circulation on Demerara Rise during the Late Cretaceous based on Nd isotopes. *Earth and Planetary Science Letters,* 327–328:111–120. **http://dx.doi.org/10.1016/j.epsl.2012.01.037**

Martin, E.E., and Scher, H.D., 2004. Preservation of seawater Sr and Nd isotopes in fossil fish teeth: bad news and good news. *Earth and Planetary Science Letters,* 220(1–2):25–39. **http://dx.doi.org/10.1016/S0012-821X(04)00030-5**

McCartney, M.S., and Donohue, K.A., 2007. A deep cyclonic gyre in the Australian–Antarctic Basin. *Progress in Oceanography,* 75(4):675–750. **http://dx.doi.org/10.1016/j.pocean.2007.02.008**

Menzies, M.A., Klemperer, S.L., Ebinger, C.J., and Baker, J., 2002. Characteristics of volcanic rifted margins. *In* Menzies, M.A., Klemperer, S.L., Ebinger, C.J., and Baker, J. (Eds.), *Volcanic Rifted Margins.* Special Paper - Geological Society of America, 362:1–14. **http://dx.doi.org/10.1130/0-8137-2362-0.1**

Meuleners, M.J., Pattiaratchi, C.B., and Ivey, G.N., 2007. Numerical modelling of the mean flow characteristics of the Leeuwin Current System. *Deep Sea Research Part II: Topical Studies in Oceanography,* 54(8–10):837–858. **http://dx.doi.org/10.1016/j.dsr2.2007.02.003**

Middleton, J.F., and Cirano, M., 2002. A northern boundary current along Australia's southern shelves: the Flinders Current. *Journal of Geophysical Research: Oceans,* 107(C9):3129. **http://dx.doi.org/10.1029/2000JC000701**

Miller, K.G., Barrera, E., Olsson, R.K., Sugarman, P. J., and Savin, S.M., 1999. Does ice drive early Maastrichtian eustasy? *Geology,* 27(9):783–786. **http://dx.doi.org/10.1130/0091-7613(1999)027<0783:DIDEME>2.3.CO;2**

Miller, K.G., Kominz, M.A., Browning, J.V., Wright, J.D., Mountain, G.S., Katz, M.E., Sugarman, P.J., Cramer, B.S., Christie-Blick, N., and Pekar, S.F., 2005. The Phanerozoic record of global sea-level change. *Science,* 310(5752):1293–1298. **http://dx.doi.org/10.1126/science.1116412**

Moiroud M., Pucéat, E., Donnadieu, Y., Bayon, G., Moriya, K., Deconinck, J.-F., and Boyet, M., 2013. Evolution of the neodymium isotopic signature of neritic seawater on a northwestern Pacific margin: new constrains on possible end-members for the composition of deep-water masses in the Late Cretaceous ocean. *Chemical Geology,* 356:160–170. **http://dx.doi.org/10.1016/j.chemgeo.2013.08.008**

Moriya, K., Wilson, P.A., Friedrich, O., Erbacher, J., and Kawahata, H., 2007. Testing for ice sheets during the mid-Cretaceous greenhouse using glassy foraminiferal calcite from the mid-Cenomanian tropics on Demerara rise. *Geology,* 35(7):615–618. **http://dx.doi.org/10.1130/G23589A.1**

Müller, R.D., Gaina, C., and Clarke, S., 2000. Seafloor spreading around Australia. *In* Veevers, J.J. (Ed.), *Billion-Year Earth History of Australia and Neighbours in Gondwanaland*: Sydney (GEMOC Press), 18–28.

Murphy, D.P., and Thomas, D.J., 2012. Cretaceous deep-water formation in the Indian sector of the Southern Ocean. *Paleoceanography,* 27(1). **http://dx.doi.org/10.1029/2011PA002198**

Norvik, M.S., 2004. *Tectonic and Stratigraphic History of the Perth Basin.* Geoscience Australia, 2004/16. **http://www.ga.gov.au/metadata-gateway/metadata/record/61374/**

Pattiaratchi, C., 2006. Surface and sub-surface circulation and water masses off Western Australia. *Bulletin of the Australian Meteorological and Oceanographic Society,* 19:95–104.

Petrizzo, M.R., 2000. Upper Turonian–lower Campanian planktonic foraminifera from southern mid–high latitudes (Exmouth Plateau, NW Australia): biostratigraphy and taxonomic notes. *Cretaceous Research,* 21(4):479–505. **http://dx.doi.org/10.1006/cres.2000.0218**

Petrizzo, M.R., 2001. Late Cretaceous planktonic foraminifera from the Kerguelen Plateau (ODP Leg 183): new data to improve the Southern Oceans biozonation. *Cretaceous Research,* 22(6):829–855. **http://dx.doi.org/10.1006/cres.2001.0290**

Powell, C.McA., Roots, S.R., and Veevers, J.J., 1988. Pre-breakup continental extension in East Gondwanaland and the early opening of the eastern Indian Ocean. *Tectonophysics,* 155(1–4):261–283. **http://dx.doi.org/10.1016/0040-1951(88)90269-7**

Ridgway, K.R., and Dunn, J.R., 2007. Observational evidence for a Southern Hemisphere oceanic supergyre. *Geophysical Research Letters,* 34(13):L13612. **http://dx.doi.org/10.1029/2007GL030392**

Robinson, S.A., Murphy, D.P., Vance, D., and Thomas, D.J., 2010. Formation of "Southern Component Water" in the Late Cretaceous: evidence from Nd-isotopes. *Geology,* 38(10):871–874. **http://dx.doi.org/10.1130/G31165.1**

Robinson, S.A., and Vance, D., 2012. Widespread and synchronous change in deep-ocean circulation in the North and South Atlantic during the Late Cretaceous. *Paleoceanography,* 27(1):PA1102. **http://dx.doi.org/10.1029/2011PA002240**

Royer, J.-Y., and Coffin, M.F., 1992. Jurassic to Eocene plate tectonic reconstructions in the Kerguelen Plateau region. *In* Wise, S.W., Jr., Schlich, R., et al., *Proceedings of the Ocean Drilling Program, Scientific Results,* 120: College Station, TX (Ocean Drilling Program), 917–928. **http://dx.doi.org/10.2973/odp.proc.sr.120.200.1992**

Schlanger, S.O., and Jenkyns, H.C., 1976. Cretaceous oceanic anoxic events: causes and consequences. *Geologie en Mijnbouw,* 55:179–184.

Sijp, W.P., and England, M.H., 2004. Effect of the Drake passage throughflow on global climate. *Journal of Physical Oceanography,* 34(5):1254–1266. **http://dx.doi.org/10.1175/1520-0485(2004)034<1254:EOT-DPT>2.0.CO;2**

Sijp, W.P., and England, M.H., 2005. Role of the Drake Passage in controlling the stability of the ocean's thermohaline circulation. *Journal of Climate,* 18(12):1957–1966. **http://dx.doi.org/10.1175/JCLI3376.1**

Sloyan, B.M., 2006. Antarctic bottom and lower circumpolar deep water circulation in the eastern Indian Ocean. *Journal of Geophysical Research: Oceans,* 111(C2):C02006. **http://dx.doi.org/10.1029/2005JC003011**

Speich, S., Blanke, B., de Vries, P., Drijfhout, S., Döös, K., Ganachaud, A., and Marsh, R., 2002. Tasman leakage: a new route in the global ocean conveyor belt. *Geophysical Research Letters,* 29(10):55-1–55-4. **http://dx.doi.org/10.1029/2001GL014586**

Speich, S., Blanke, B., and Cai, W., 2007. Atlantic meridional overturning circulation and the Southern Hemisphere supergyre. *Geophysical Research Letters,* 34(23):L23614. **http://dx.doi.org/10.1029/2007GL031583**

Stoll, H.M., and Schrag, D.P., 2000. High resolution stable isotope records from the upper Cretaceous of Italy and Spain: glacial episodes in a greenhouse planet? *Geological Society of America Bulletin,* 112(2):308–319. **http://dx.doi.org/10.1130/0016-7606(2000)112<0308:HRSIRF>2.3.CO;2**

Thibault, N., Husson, D., Harlou, R., Gardin, S., Galbrun, B., Huret, E., and Minoletti, F., 2012. Astronomical calibration of upper Campanian–Maastrichtian carbon isotope events and calcareous plankton biostratigraphy in the Indian Ocean (ODP Hole 762C): implication for the age of the Campanian–Maastrichtian boundary. *Palaeogeography, Palaeoclimatology., Paleoecology,* 337–338:52–71. **http://dx.doi.org/10.1016/j.palaeo.2012.03.027**

Thierstein, H.R., 1974. Calcareous nannoplankton—Leg 26, Deep Sea Drilling Project. *In* Davies, T.A., Luyendyk, B.P., et al., *Initial Reports of the Deep Sea Drilling Project,* 26: Washington, DC (U.S. Govt. Printing Office), 619–667. **http://dx.doi.org/10.2973/dsdp.proc.26.128.1974**

Tikku, A.A., and Cande, S.C., 1998. The oldest magnetic anomalies in the Australian-Antarctic Basin: are they isochrons? *Journal of Geophysical*

Research: Solid Earth, 104(B1):661–677. **http://dx.doi.org/10.1029/1998JB900034**

Tikku, A.A., and Cande, S.C., 2000. On the fit of Broken Ridge and Kerguelen Plateau. *Earth and Planetary Science Letters,* 180(1–2):117–132. **http://dx.doi.org/10.1016/S0012-821X(00)00157-6**

Toggweiler, J.R., and Samuels, B., 1995. Effect of Drake Passage on the global thermohaline circulation. *Deep Sea Research, Part I,* 42(4):477–500. **http://dx.doi.org/10.1016/0967-0637(95)00012-U**

Toggweiler, J.R., and Samuels, B., 1998. On the ocean's large-scale circulation near the limit of no vertical mixing. *Journal of Physical Oceanography,* 28(9):1832–1852. **http://dx.doi.org/10.1175/1520-0485(1998)028<1832:OTOSLS>2.0.CO;2**

Totterdell, J.M., and Mitchell, C.H. (Eds.), 2009. *Bight Basin Geological Sampling and Seepage Survey: R/V* Southern Surveyor Survey *SS01/2007.* Geoscience Australia, 2009/24. **http://www.ga.gov.au/metadata-gateway/metadata/record/gcat_68689**

Totterdell, J.M., Struckmeyer, H.I.M., Boreham, C.J., Mitchell, C.H., Monteil, E., and Bradshaw, B.E., 2008. Mid–Late Cretaceous organic-rich rocks from the eastern Bight Basin: implications for prospectivity. *In* Blevin, J.E., Bradshaw, B.E., and Uruski, C. (Eds.), *Eastern Australasian Basins Symposium III.* Petroleum Exploration Society of Australia Special Publication, 137–158.

van Sebille, E., England, M.H., Zika, J.D., and Sloyan, B.M., 2012. Tasman leakage in a fine-resolution ocean model. *Geophysical Research Letters,* 39(6):L06601. **http://dx.doi.org/10.1029/2012GL051004**

Voigt, S., Jung, C., Friedrich, O., Frank, M., Teschner, C., and Hoffmann, J., 2013. Tectonically restricted deep-ocean circulation at the end of the Cretaceous greenhouse. *Earth and Planetary Science Letters,* 369–370:169–177. **http://dx.doi.org/10.1016/j.epsl.2013.03.019**

Waite, A.M., Thompson, P.A., Pesant, S., Feng, M., Beckley, L.E., Domingues, C.M., Gaughan, D., Hanson, C.E., Holl, C.M., Koslow, T., Meuleners, M., Montoya, J.P., Moore, T., Muhling, B.A., Paterson, H., Rennie, S., Strzelecki, J., and Twomey, L., 2007. The Leeuwin Current and its eddies: an introductory overview. *Deep Sea Research Part II: Topical Studies in Oceanography,* 54(8–10):789–796. **http://dx.doi.org/10.1016/j.dsr2.2006.12.008**

White, L.T., Gibson, G.M., and Lister, G.S., 2013. A reassessment of paleogeographic reconstructions of eastern Gondwana: bringing geology back into the equation. *Gondwana Research,* 24(3–4):984–998. **http://dx.doi.org/10.1016/j.gr.2013.06.009**

Williams, S.E., Whittaker, J.M., and Müller, R.D., 2011. Full-fit, palinspastic reconstruction of the conjugate Australian-Antarctic margins. *Tectonics,* 30(6):TC6012. **http://dx.doi.org/10.1029/2011TC002912**

Wunsch, C., 2002. What is the thermohaline circulation? *Science,* 298(5596):1179–1181. **http://dx.doi.org/10.1126/science.1079329**

Zheng, X.-Y., Jenkyns, H.C., Gale, A.S., Ward, D.J., and Henderson, G.M., 2013. Changing ocean circulation and hydrothermal inputs during oceanic anoxic Event 2 (Cenomanian–Turonian): evidence from Nd-isotopes in the European shelf sea. *Earth and Planetary Science Letters,* 375:338–348. **http://dx.doi.org/10.1016/j.epsl.2013.05.053**

Table T1. Operations plan for primary proposed sites, Expedition 369. EPSP = Environmental Protection and Safety Panel. RCB = rotary core barrel, APC = advanced piston corer, XCB = extended core barrel. FMS = Formation MicroScanner, VSI = Versatile Seismic Imager.

Site	Location (Latitude Longitude)	Seafloor depth (mbrf)	Operations description	Transit (days)	Drilling/ Coring (days)	Logging (days)
Hobart			Begin expedition 5.0	Port call days		
			Transit ~1047 nmi to WCED-4A (APL site) @ 10.5 kt	4.7		
WCED-4A (APL site)	34°1.6407'S	3046	Hole A - RCB to 570 mbsf; wireline log with triple combo and FMS-sonic	0	4.7	0.7
EPSP approved	127°57.7604'E					
to 570 mbsf						
			Subtotal days on-site: 5.4			
			Transit ~837 nmi to MBAS-8C @ 10.5 kt	3.3		
MBAS-8D	33°7.2324'S	3901	Hole A - APC to 300 mbsf	0	2.4	0
EPSP approved	113°5.4675'E		Hole B - APC/XCB to 800 mbsf	0	6.3	0
to 1200 mbsf			Hole C - Drill-in casing to 370 mbsf; RCB from 370 to 1100 mbsf; log with triple combo, FMS-sonic, and VSI	0	10.1	1.9
			Subtotal days on-site: 20.7			
			Transit ~51 nmi to MBAS-4B @ 10.5 kt	0.2		
MBAS-4B	33°47.7984'S	2801	Hole A - APC to 110 mbsf; XCB to 730; log with FMS-sonic, triple combo, and VSI	0	5.2	1.7
EPSP approved	112°28.1406'E		Hole B - APC/XCB to 490 mbsf	0	3.4	0
to 880 mbsf						
			Subtotal days on-site: 10.3			
			Transit ~98 nmi to MBAS-9A @ 10.5 kt	0.4		
MBAS-9A	33°16.1886'S	861	Hole A - APC/XCB to 364 mbsf	0	1.7	0
EPSP approved	114°19.3668'E		Hole B - APC/XCB to 364 mbsf	0	1.4	0
to 1200 mbsf			Hole C - Drill down to ~350 mbsf; RCB to 1200 mbsf; log with triple combo, FMS-sonic, and VSI	0	5.5	2
			Subtotal days on-site: 10.7			
			Transit ~103 nmi to Fremantle @ 10.5 kt	0.4		
Fremantle			End expedition	8.9	40.8	6.3

Port call:	5	Total operating days:	56
Subtotal on-site:	47.1	Total expedition:	61

Table T2. Operations plan for alternate proposed sites, Expedition 369. EPSP = Environmental Protection and Safety Panel. APC = advanced piston corer, XCB = extended core barrel, RCB = rotary core barrel, HLAPC = half-length APC. FMS = Formation MicroScanner, VSI = Versatile Seismic Imager.

Site	Location (Latitude Longitude)	Seafloor depth (mbrf)	Operations description	Drilling/ Coring (days)	Logging (days)
MBAS-8B	33°7.1400'S	3901	Hole A - APC to 300 mbsf	2.4	0
EPSP	113°5.4648'E		Hole B - APC to 300 mbsf	1.90	0
to 1200 mbsf			Hole C - APC/XCB to 800 mbsf	6.30	0
			Hole D - Drill down to ~750 mbsf; RCB to 1060 mbsf; log with triple combo and FMS-sonic	5.70	1.7
			Subtotal days on-site: 18		
MBAS-4C	33°47.6076'S	2801	Hole A - APC to 150 mbsf	1.50	0
EPSP	112°29.1348'E		Hole B - APC to 150 mbsf	1.00	0
to 880 mbsf			Hole C - APC/XCB to 520 mbsf	3.7	0
			Hole D - Drill down to ~470 mbsf; RCB to 880 mbsf; log with triple combo and FMS-sonic	6	1.5
			Subtotal days on-site: 13.6		
MBAS-6A	33°52.9524'S	1211	Hole A - APC/HLAPC to 200 mbsf	1.2	0
EPSP	114°13.4940'E		Hole B - APC/HLAPC to 200 mbsf	0.8	0
to 1200 mbsf			Hole C - APC/XCB to 400 mbsf	1.9	0
			Hole D - Drill-in a reentry system with 10-3/4" casing to 350 mbsf	2.1	0
			Hole D - RCB from 400 to 1200 mbsf; log with triple combo, FMS-sonic, and VSI	6.6	1.8
			Subtotal days on-site: 14.4		
MBAS-3C	33°54.7944'S	3131	Hole A - APC to 150 mbsf	1.4	0
EPSP	113°12.7236'E		Hole B - APC to 150 mbsf	0.9	0
to 1500 mbsf			Hole C - APC/XCB to 800 mbsf	5.7	0
			Hole D - Drill-in a reentry system with 10-3/4" casing to 400 mbsf	2.6	0
			Hole D - RCB from 400 - 1500 mbsf and log with triple combo, FMS sonic, and VSI	12.8	2.2
			Subtotal days on-site: 25.5		
MBAS-5B	34°23.9118'S	2711	Hole A - APC to 200 mbsf	1.6	0
EPSP	112°49.0362'E		Hole B - APC to 200 mbsf	1.1	0
to 750 mbsf			Hole C - APC/XCB to 468 mbsf	3.2	0
			Hole D - Drill down to ~450 mbsf; RCB to 750 mbsf; log with triple combo and FMS-sonic	4.3	1.5
			Subtotal days on-site: 11.6		

Figure F1. Late Cenomanian and middle Eocene paleogeographic maps (Hay et al., 1999) showing the location of Site 258 and select deep-sea sites yielding reliable oxygen isotope data from Cretaceous sediments. GAB = Great Australian Bight, TDP = Tanzania Drilling Project.

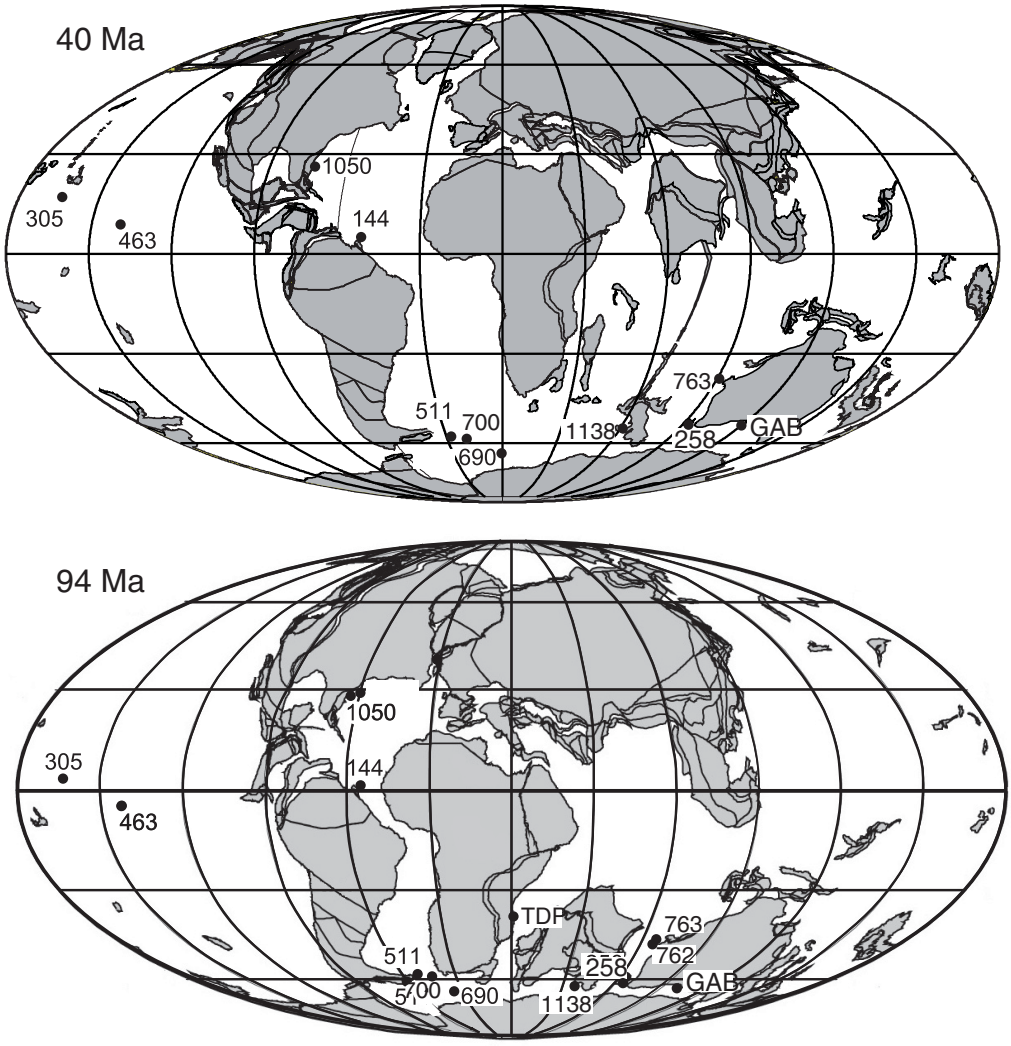

Figure F2. A. Regional context of the NP and MB, including location of the major reflection seismic profiles, DSDP sites, and proposed sites. PB = Perth Basin, LB = Leeuwin Block, YS = Yallingup shelf. B. Location of Site WCED-4A in the Great Australian Bight. ODP Leg 182 sites and petroleum exploration wells, as well as 2-D seismic lines are also shown.

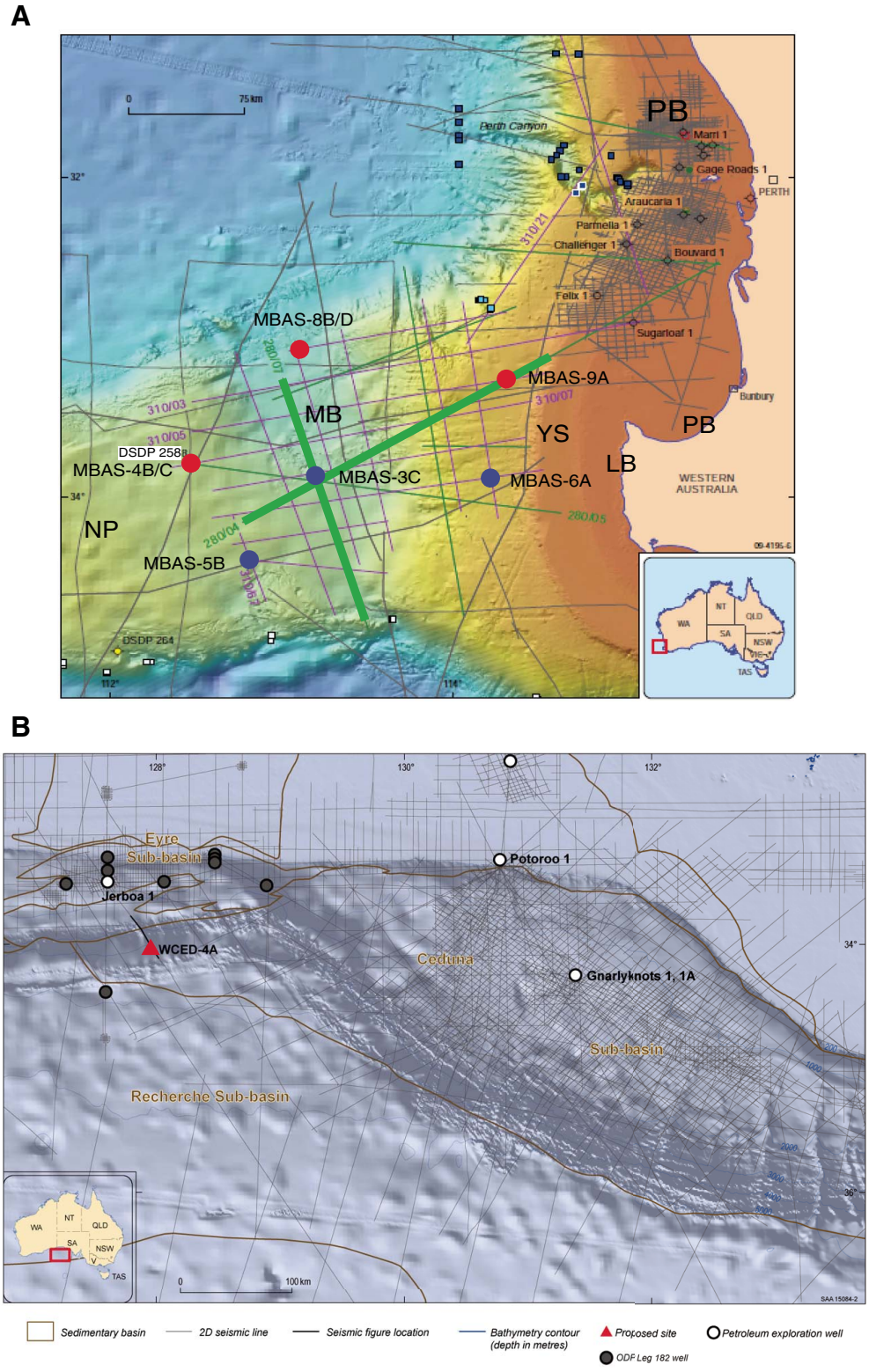

Figure F3. A. TOC vs. Rock-Eval pyrolysis parameter S2 for selected dredge samples recovered by Geoscience Australia in 2007 in the Great Australian Bight. Modified after Totterdell et al. (2008). B. Location of dredge sites, which are 10 and 15 km north-northwest of proposed Site WCED-4A. Modified after Totterdell et al. (2008). C. Black shale recovered from dredge Site DR16 (see B) and dated as latest Cenomanian–earliest Turonian. D. Gas chromatograph of saturated hydrocarbons from dredge Site DR17 (see B). The assemblage of molecular biomarkers in this sample is representative of the others and is consistent with algal organic matter as a major source and preservation in an anoxic depositional setting. Modified after Boreham (2009). FID = flame ionization detector. HI = hydrogen index, Pr = pristane, Ph = phytane.

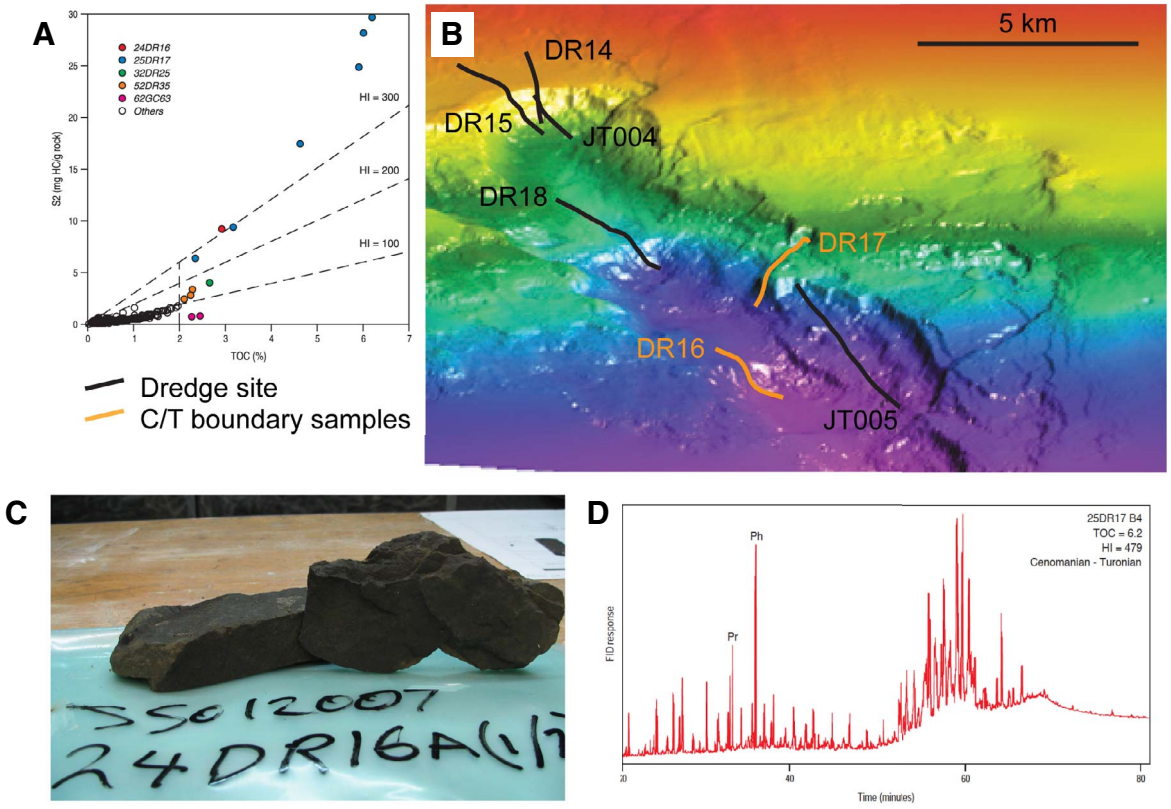

Figure F4. Ocean currents in the modern ocean surrounding Australia. Orange = surface currents, green = intermediate currents, blue = deep ocean currents. Yellow circles = primary Sites WCED-4A, MBAS-8D, MBAS-4B, and MBAS-9A.

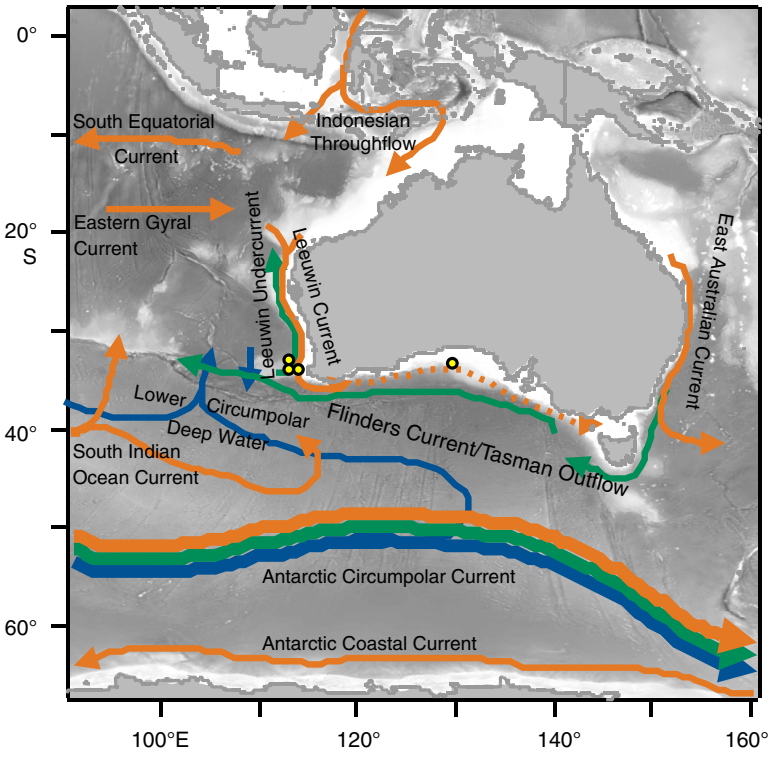

Figure F5. Stable isotope data from Holes 258 and 258A with few data from Huber et al. (1995) plotted and new unpublished data using revised calcareous nannofossil and planktonic foraminiferal biostratigraphic zonal and age assignments. Cored intervals: black = recovered core, white = unrecovered core, cross-hatched pattern = intervals drilled without coring. VPDB = Vienna Peedee belemnite. *Gl. prairiehillensis = Globigerinelloides prairiehillensis, Gx = Globoheterohelix, Gl. linneiana = Globotruncana linneiana, Ar = Archaeoglobigerina.*

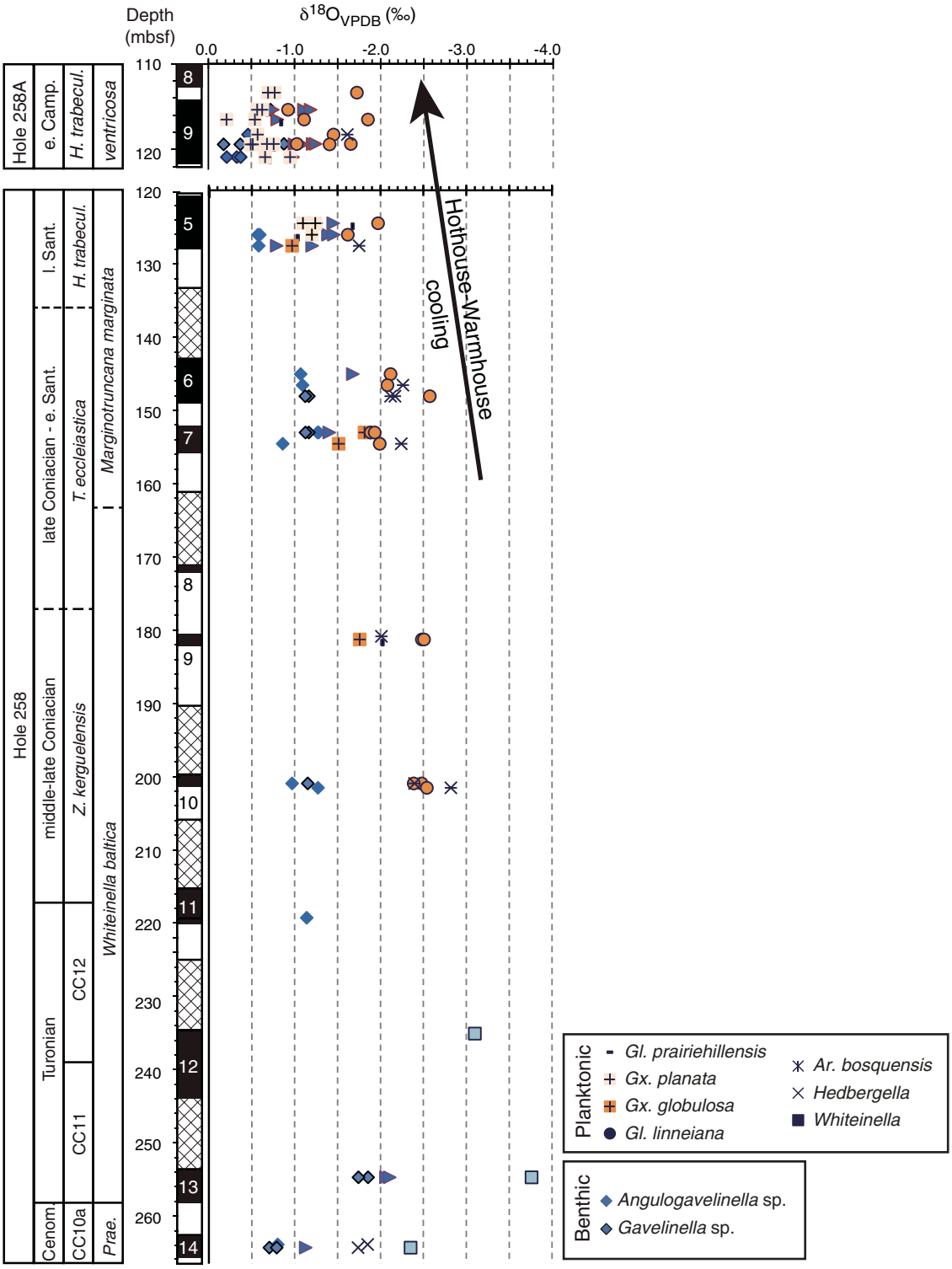

Figure F6. Comparison of frosty and glassy planktonic foraminiferal shell wall preservation, Site 258 samples. A, B. *Globigerinelloides bollii* (Santonian), showing external umbilical view and interior view of broken penultimate chamber (DSDP 26-258-5-1, 103–106 cm). C, D. *Muricohedbergella delrioensis* (Cenomanian), showing external umbilical view and interior view of broken penultimate chamber (DSDP 26-258-14-1, 83–86 cm).

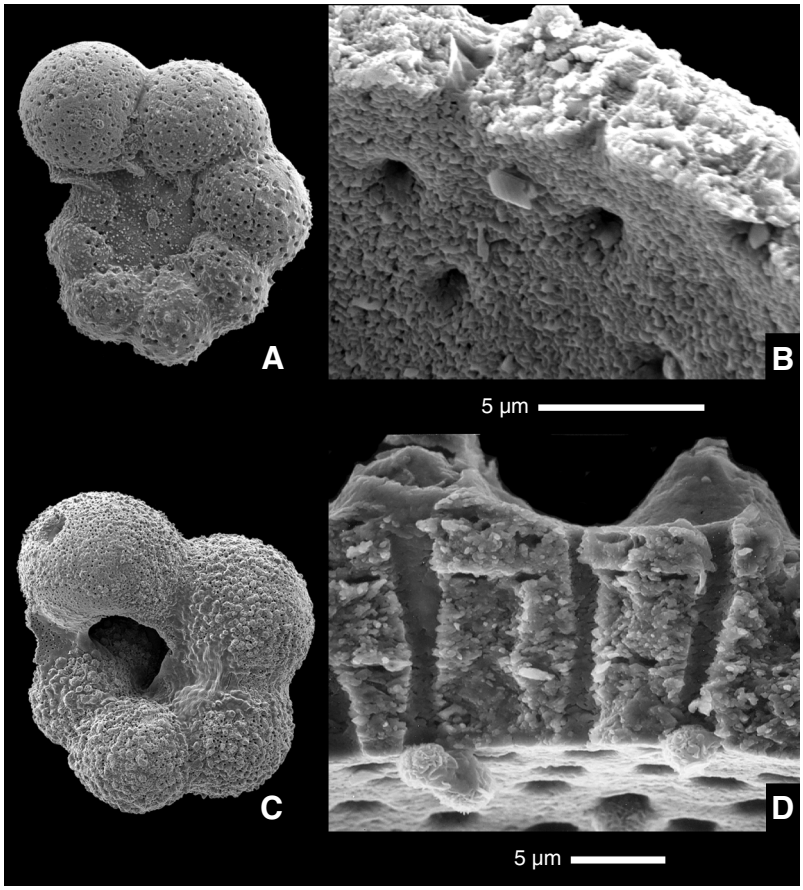

Figure F7. Southwest to northeast section across the Mentelle Basin (Profile 280/04; see Figure **F2** for location). Stratigraphic units colored as in Figure **F9** (adapted from Borissova, 2002).

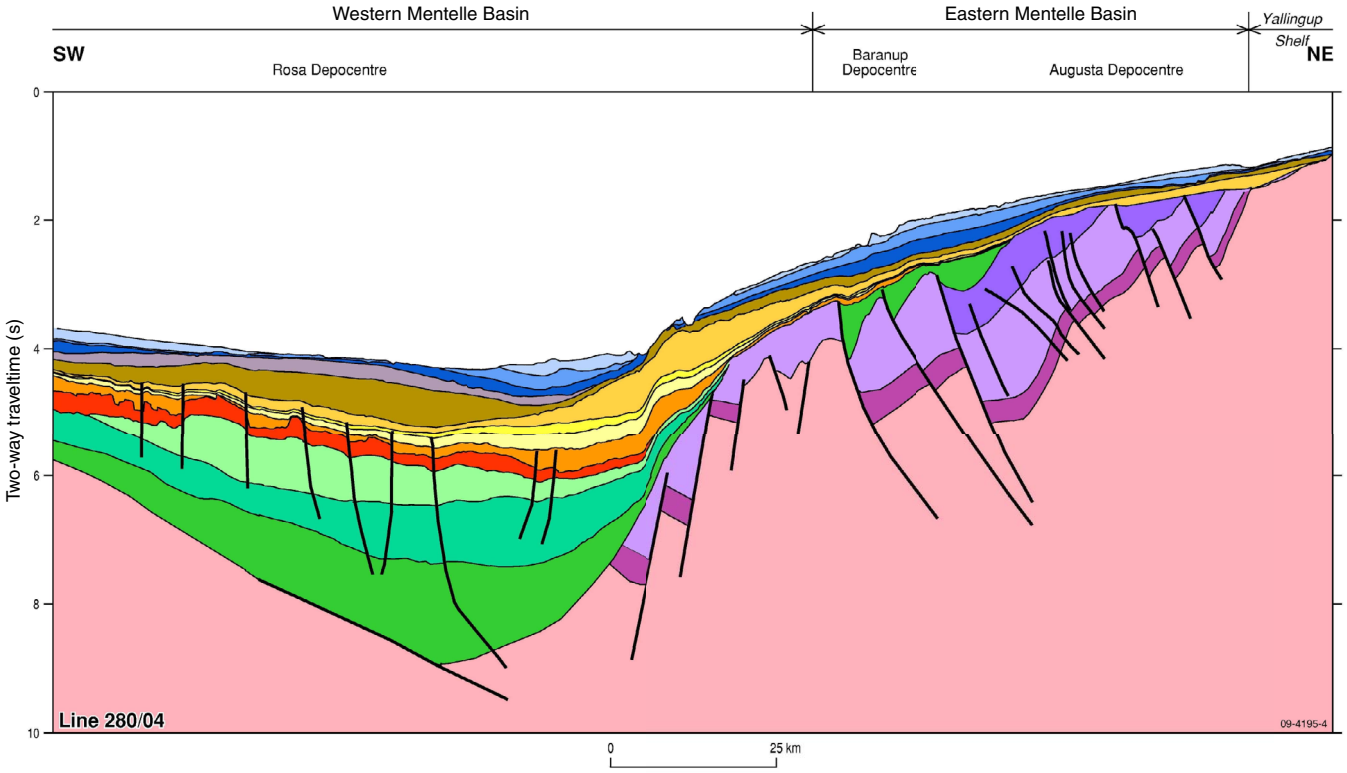

Figure F8. North to south section across the Mentelle Basin (Profile 280/07; see Figure **F2** for location). Stratigraphic units colored as in Figure **F9** (adapted from Borissova, 2002).

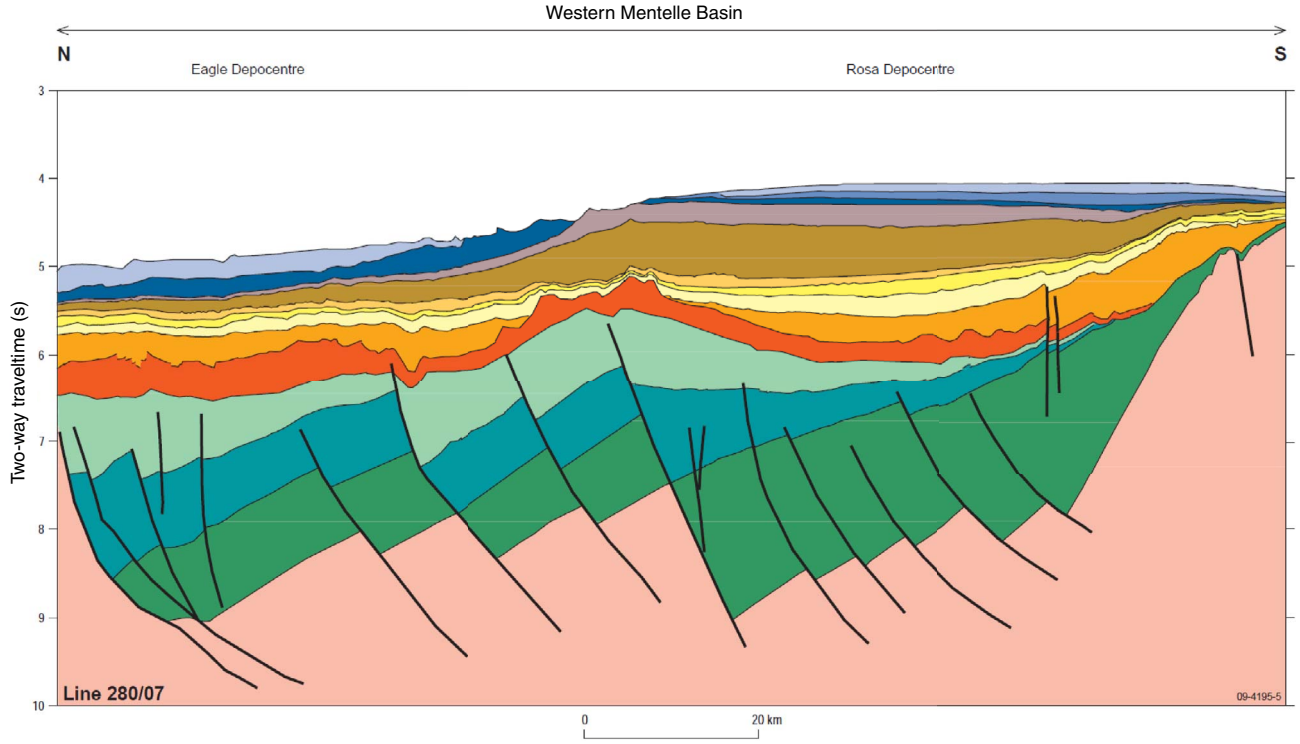

Figure F9. Stratigraphic column for the Mentelle and adjacent Perth Basins. Sst = sandstone, Fm = formation.

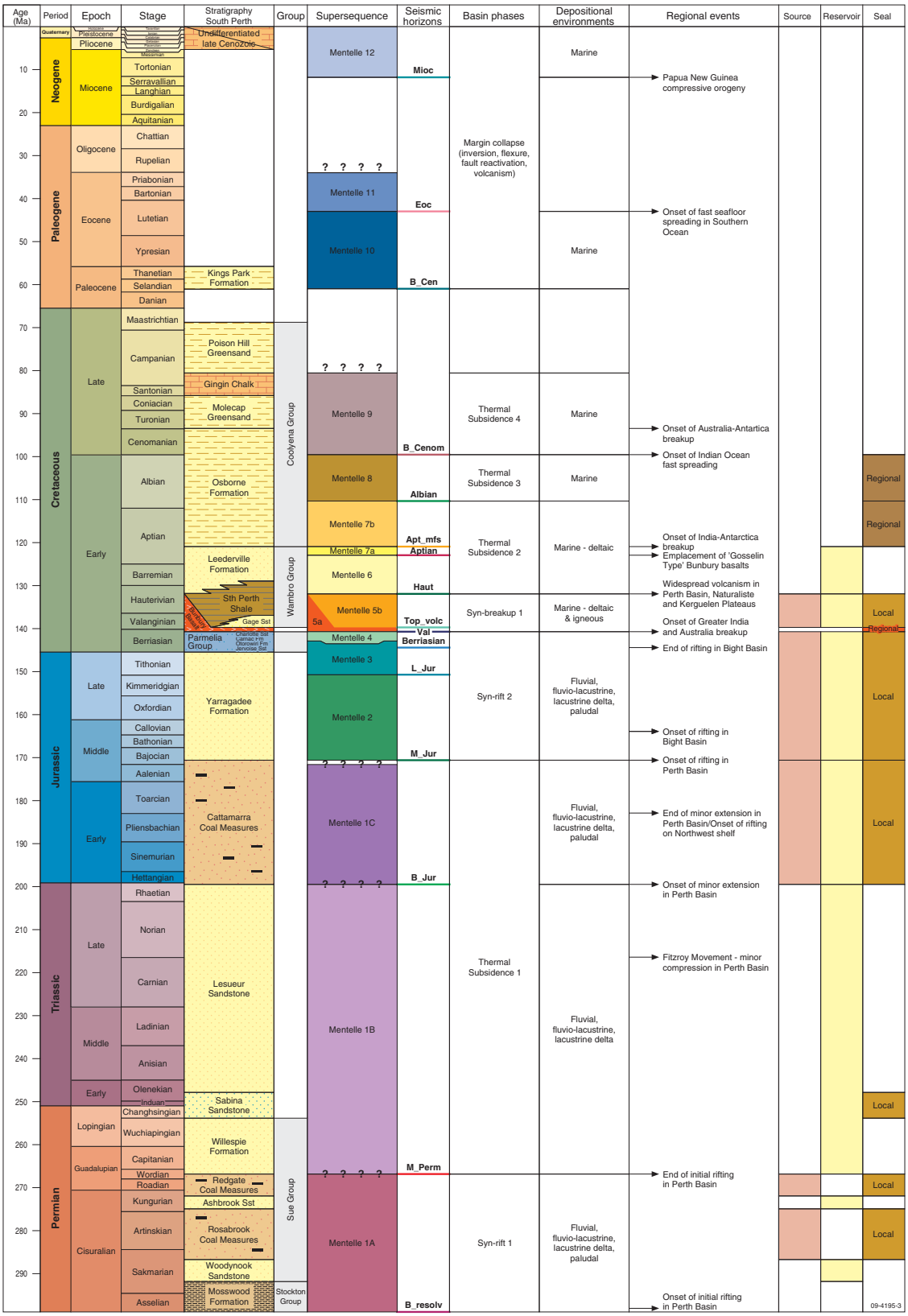

Site summaries

Site WCED-4A

Priority:	Primary
Position:	34°1.6407′S, 127°57.7604′E
Water depth (m):	3035
Target drilling depth (mbsf):	570
Approved maximum penetration (mbsf):	570
Survey coverage (track map; seismic profile):	Figure **AF1**
Objective(s):	Core and recover OAE 2, which extends its characterization in high latitudes.
Drilling program:	RCB (single hole) to target depth
Logging/Downhole measurements program:	Triple combo, FMS-sonic
Nature of rock anticipated:	90 m of Cenozoic carbonate sediment overlaying 480 m of Cenomanian–Turonian mudstone (including OAE 2)

Site MBAS-8D

Priority:	Primary
Position:	33°7.2324′S, 113°5.4675′E
Water depth (m):	3890
Target drilling depth (mbsf):	1100
Approved maximum penetration (mbsf):	1200
Survey coverage (track map; seismic profile):	Figures **AF2**, **AF3**
Objective(s):	This site targets sediments deposited during the collapse of the Cretaceous warmhouse (including OAE 2), which is an undersampled interval in the $\delta^{18}O$ record. The site also samples a series of erosional features, which will provide insight into the Cretaceous and Cenozoic paleoceanography of the southwest corner of Australia.
Drilling program:	Double APC, single XCB followed by installation of ~370 m of casing, and RCB coring to target depth
Logging/Downhole measurements program:	APCT-3 measurements in one hole; triple combo, FMS-sonic, and VSI
Nature of rock anticipated:	~370 m of Cenozoic sedimentary drifts and erosional features; 166 m Albian ferruginous clay; 663 m shallow marine or deltaic sediments, with possible basalt or volcaniclastic sediments at base

Site MBAS-4B

Priority:	Primary
Position:	33°47.7984′S, 112°28.1406′E (adjacent to Site 258)
Water depth (m):	2790
Target drilling depth (mbsf):	730
Approved maximum penetration (mbsf):	880
Survey coverage (track map; seismic profile):	Figures **AF2**, **AF4**
Objective(s):	This site will capture the depositional history prior to and during OAEs 1 and 2. Coring will continue down to the extrusive basalt layer at the Valanginian unconformity.
Drilling program:	Double APC, single XCB
Logging/Downhole measurements program:	APCT-3 measurements in one hole; triple combo, FMS-sonic, and VSI
Nature of rock anticipated:	114 m Miocene–recent calcareous ooze; 166 m Cenomanian–early Campanian chalk; 234 m Valanginian–middle Albian volcanic sediments; 260 m shallow marine sediments and possible basalt

Site MBAS-9A

Priority:	Primary
Position:	33°16.1886′S, 114°19.3668′E
Water depth (m):	850
Target drilling depth (mbsf):	1200
Approved maximum penetration (mbsf):	1200
Survey coverage (track map; seismic profile):	Figures **AF2**, **AF5**
Objective(s):	This site is a stratigraphic calibration well on the continental slope (eastern Mentelle Basin) with the principal goal to define the sediment age beneath the Valanginian unconformity that records prebreakup depositional history in the region prior to the final rifting of Greater India and Antarctica.
Drilling program:	Double APC, single XCB followed by RCB coring to target depth
Logging/Downhole measurements program:	APCT-3 measurements in one hole; triple combo, FMS-sonic, and VSI
Nature of rock anticipated:	200 m of Cenozoic chalk; 164 m of Aptian to Valanginian deltaic sediments; 836 m of Jurassic fluviodeltaic sandstone and conglomerates

Site MBAS-8B

Priority:	Alternate
Position:	33°7.1400′S, 113°5.4648′E
Water depth (m):	2990
Target drilling depth (mbsf):	1060
Approved maximum penetration (mbsf):	1200
Survey coverage (track map; seismic profile):	Figures **AF2**, **AF3**
Objective(s):	This site is an alternate to Site MBAS-8D with the same objectives.
Drilling program:	Triple APC, single XCB to 800 mbsf, then RCB to total depth
Logging/Downhole measurements program:	APCT-3 measurements in one hole; triple combo, FMS-sonic
Nature of rock anticipated:	~370 m of Cenozoic sedimentary drifts and erosional features; 166 m of Albian ferruginous clay; 663 m shallow marine or deltaic sediments, with possible basalt or volcaniclastic sediments at base

Site MBAS-4C

Priority:	Alternate
Position:	33°47.6076′S, 112°29.1348′E
Water depth (m):	2790
Target drilling depth (mbsf):	880
Approved maximum penetration (mbsf):	880
Survey coverage (track map; seismic profile):	Figures **AF2**, **AF4**
Objective(s):	This site is an alternate to Site MBAS-4B with the same objectives.
Drilling program:	Triple APC, single XCB to 520 mbsf, then RCB to total depth
Logging/Downhole measurements program:	APCT-3 measurements in one hole; triple combo, FMS-sonic
Nature of rock anticipated:	114 m of Miocene–recent calcareous ooze; 166 m of Cenomanian–early Campanian chalk; 234 m of Valanginian–middle Albian volcanic sediments; 260 m of shallow marine sediments and possible basalt

Site MBAS-6A

Priority:	Alternate
Position:	33°52.9524′S, 114°13.4940′E
Water depth (m):	1200
Target drilling depth (mbsf):	1200
Approved maximum penetration (mbsf):	1200
Survey coverage (track map; seismic profile):	Figures **AF2**, **AF6**
Objective(s):	This is a stratigraphic calibration site on the continental slope (eastern Mentelle Basin) with the principal goal to define the sediment age and provenance beneath the Valanginian unconformity that records prebreakup depositional history in the region prior to the final rifting of Greater India and Antarctica and the provenance of the sediments. It will also provide information for shallow paleoceanography studies.
Drilling program:	Triple APC, single XCB to 400 mbsf, install casing to 350 mbsf, then RCB to total depth
Logging/Downhole measurements program:	APCT-3 measurements in one hole; triple combo, FMS-sonic, and VSI
Nature of rock anticipated:	57 m of Cenozoic chalk; 62 m of Aptian limestone with sandstone at base; 62 m of Aptian shallow marine sediments (sandstone/silt/shale); 93 m of Valanginian sandstone; 826 m of Jurassic fluviodeltaic mainly sandstone with some shale

Site MBAS-3C

Priority:	Alternate
Position:	33°54.7944′S, 113°12.7236′E
Water depth (m):	3120
Target drilling depth (mbsf):	1500
Approved maximum penetration (mbsf):	1500
Survey coverage (track map; seismic profile):	Figures **AF2**, **AF7**
Objective(s):	This site is close to the depocenter of the western Mentelle Basin and is targeted to sample the Valanginian breakup unconformity and the postbreakup succession, including the Aptian–Albian black shales/claystones.
Drilling program:	Triple APC, single XCB to 400 mbsf, install casing to 400 mbsf, then RCB to total depth
Logging/Downhole measurements program:	APCT-3 measurements in one hole; triple combo, FMS-sonic, and VSI
Nature of rock anticipated:	Thin Cenozoic sediments underlain by thick Aptian–Albian claystone over glauconitic sandstone to the Valanginian unconformity

Site MBAS-5B

Priority:	Alternate
Position:	34°23.9118′S, 112°49.0362′E
Water depth (m):	2700
Target drilling depth (mbsf):	750
Approved maximum penetration (mbsf):	750
Survey coverage (track map; seismic profile):	Figures **AF2**, **AF8**
Objective(s):	This site targets the basement on the southern margin of the Naturaliste Plateau and to test a very condensed Albian to Cenozoic succession, which will allow us to define the southward extent of sediments deposited during OAEs 1 and 2 and any $\delta^{18}O$ changes associated with this distal position.
Drilling program:	Triple APC, XCB to 468 mbsf, then RCB to total depth
Logging/Downhole measurements program:	APCT-3 measurements in one hole; triple combo, FMS-sonic
Nature of rock anticipated:	257 m of Miocene–Cenozoic coccolith ooze; 123 m of Turonian–Campanian chalk with chert bands; 88 m of Albian clay/chalk; 282 m of Valanginian basalt

Figure AF1. Track map and seismic profile, primary Site WCED-4A. The dredge sites where organic-rich Cenomanian–Turonian black shales were recovered are also shown.

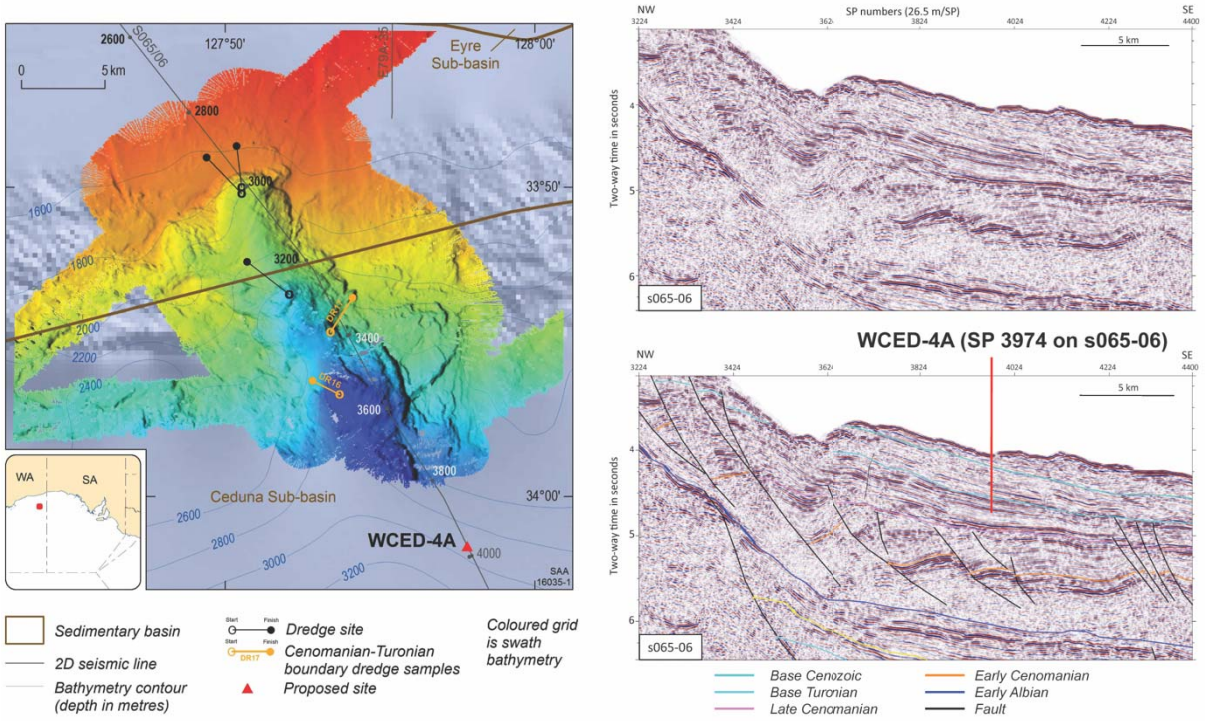

Figure AF2. Regional track map for MB and NP sites.

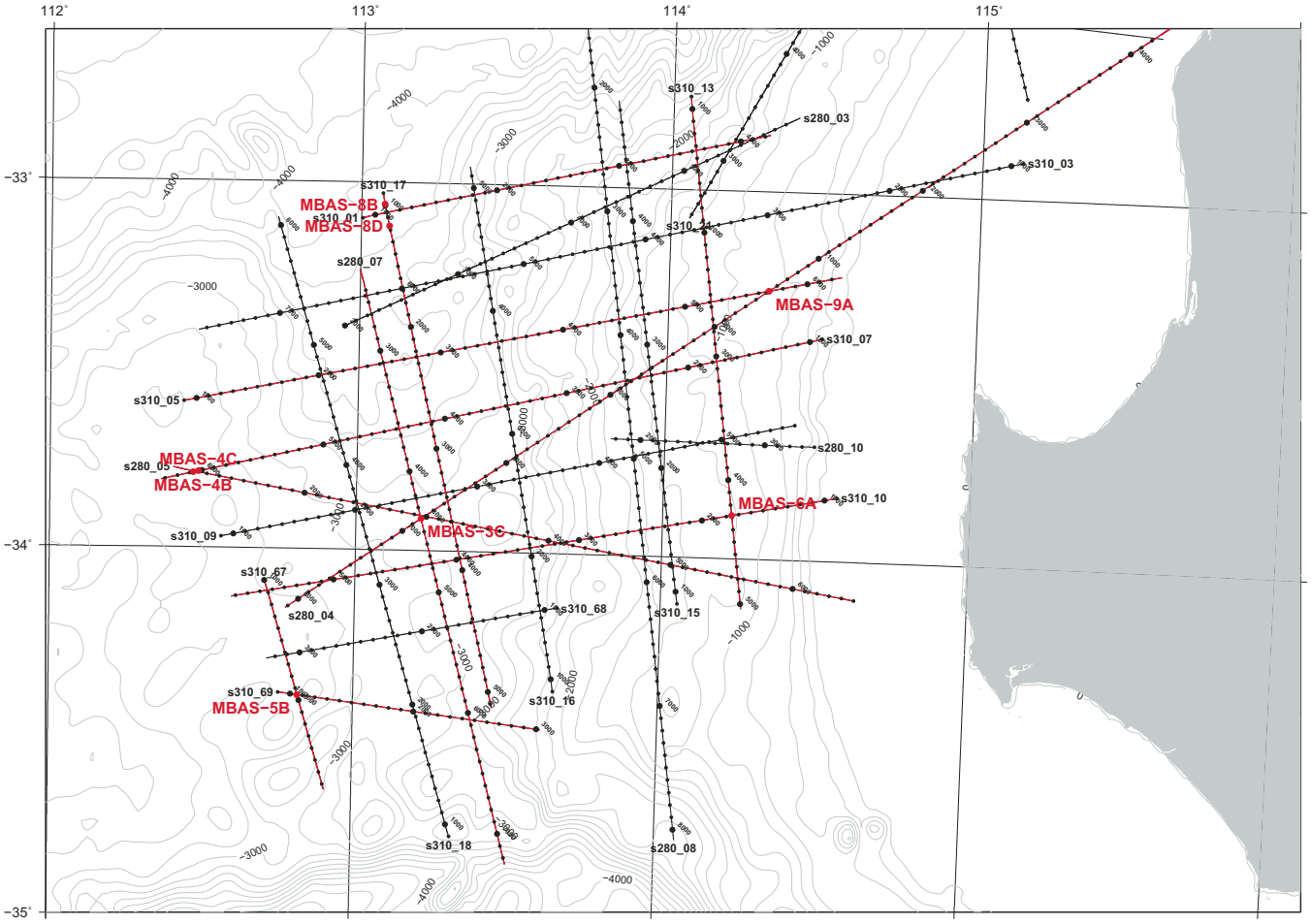

Figure AF3. Track map and seismic profile, primary Site MBAS-8D and alternate Site MBAS-8B.

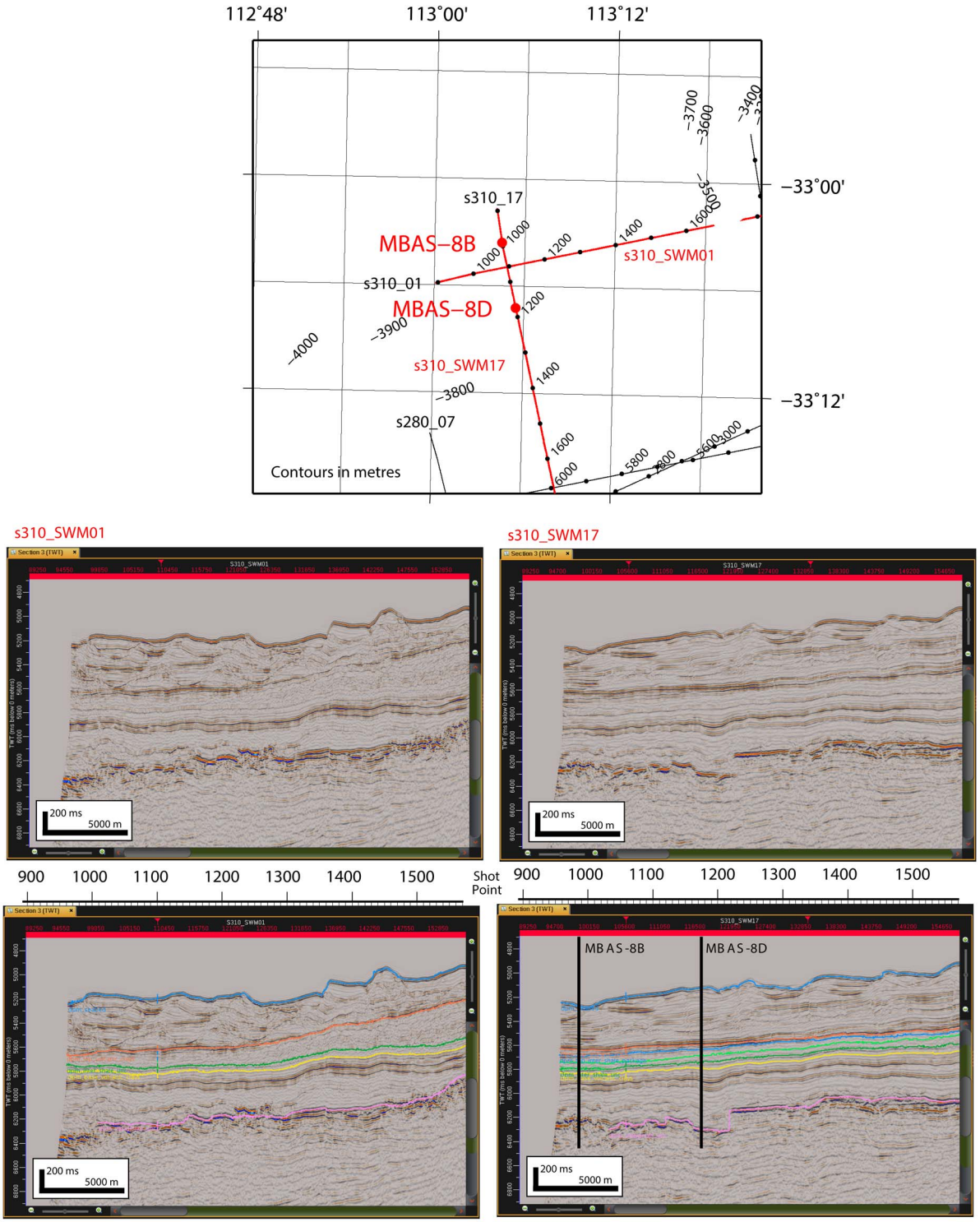

Key Interpreted Horizons
cyan - base Paleogene deep-marine chalk (Mentelle 10 & 11) and Cretaceous coccolith-rich chalk (Mentelle 9)
top Albian/Aptian shales (Mentelle 7a, 7b & 8)
yellow - base shale
top detrital sandstone/glauconitic clay (Mentell 5b & 6)
orange - top volcanic cone/carbonate reef (Mentelle 5a?)
purple - top Valanginian basalt (Mentelle 5a)

Figure AF4. Track map and seismic profile, primary Site MBAS-4B and alternate Site MBAS-4C.

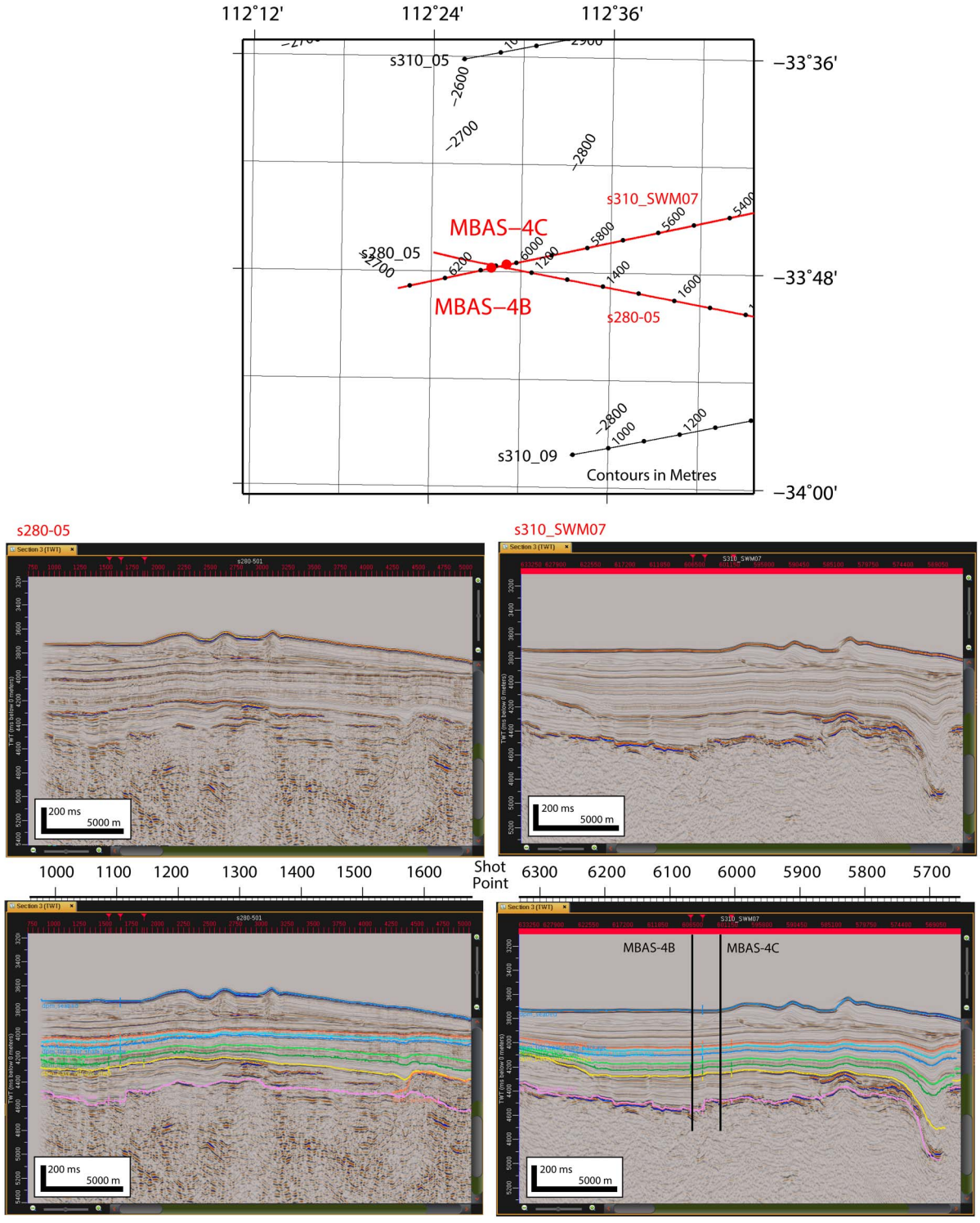

Key Interpreted Horizons
cyan - base Paleogene deep-marine chalk and
Cretaceous coccolith-rich chalk (Mentelle 9, 10 & 11Mentelle 9)
top Albian/Aptian shales (Mentelle 7a, 7b & 8)
yellow - base shale
top detrital sandstone/glauconitic clay (Mentell 5b & 6)
purple - top Valanginian basalt (Mentelle 5a)

Figure AF5. Track map and seismic profile, primary Site MBAS-9A.

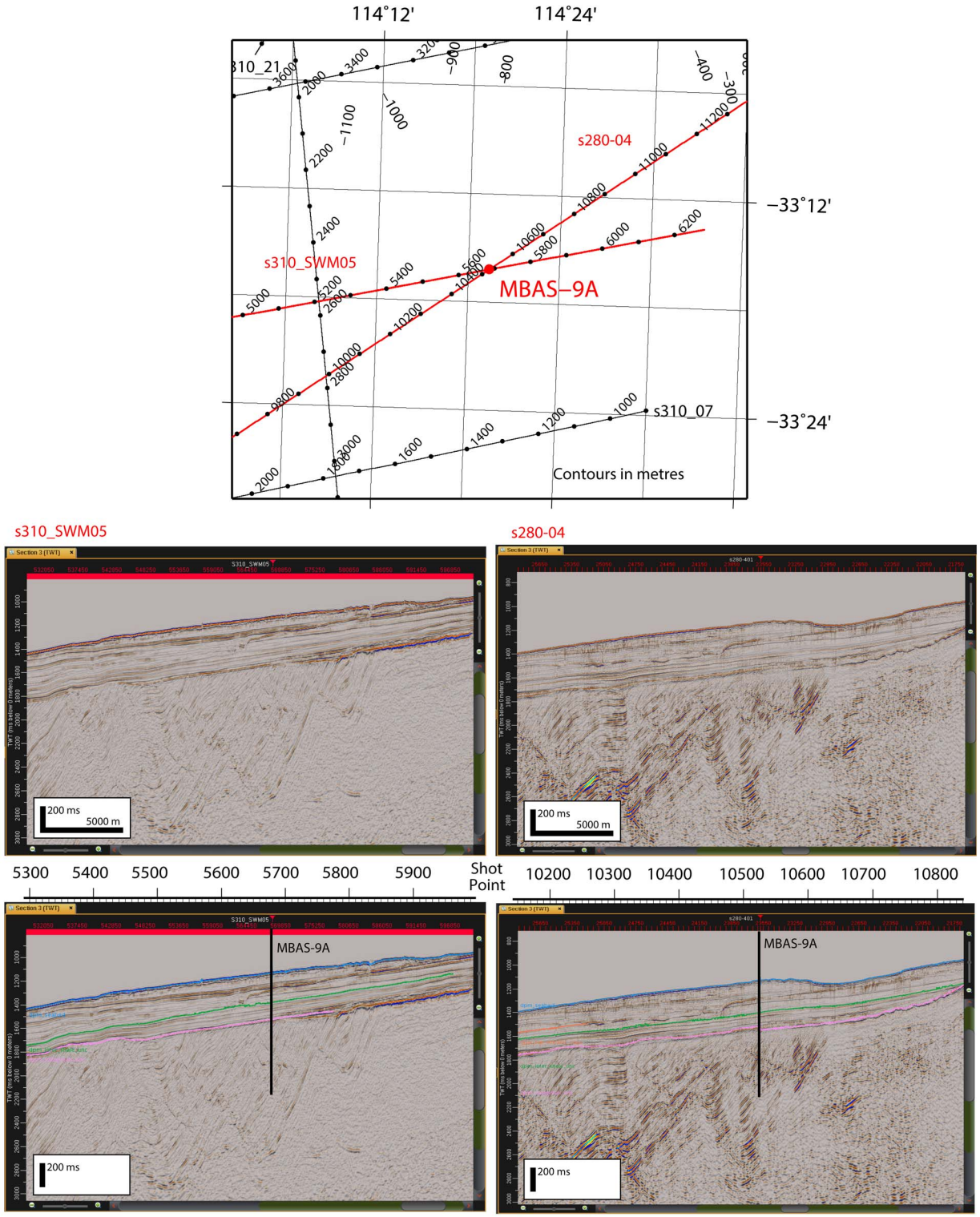

Key Interpreted Horizons
green - inter Albian/Aptian shales unconformity (Mentelle 7a, 7b)

purple - top Valanginian unconformity (Mentelle 4)
undifferentiated Jurassic/Triassic(?)

Figure AF6. Track map and seismic profile, alternate Site MBAS-6A.

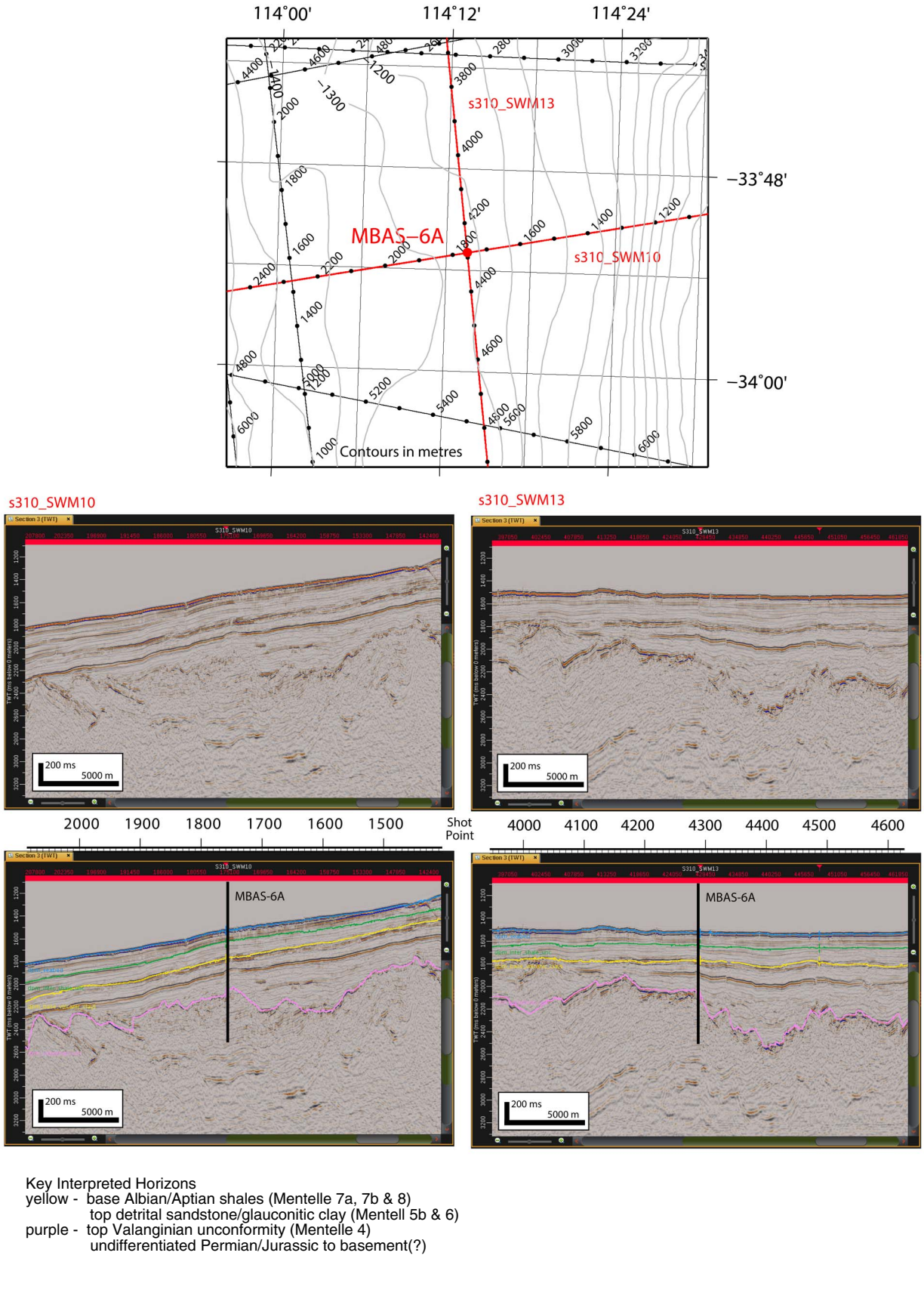

Key Interpreted Horizons
yellow - base Albian/Aptian shales (Mentelle 7a, 7b & 8)
top detrital sandstone/glauconitic clay (Mentell 5b & 6)
purple - top Valanginian unconformity (Mentelle 4)
undifferentiated Permian/Jurassic to basement(?)

Figure AF7. Track map and seismic profile, alternate Site MBAS-3C.

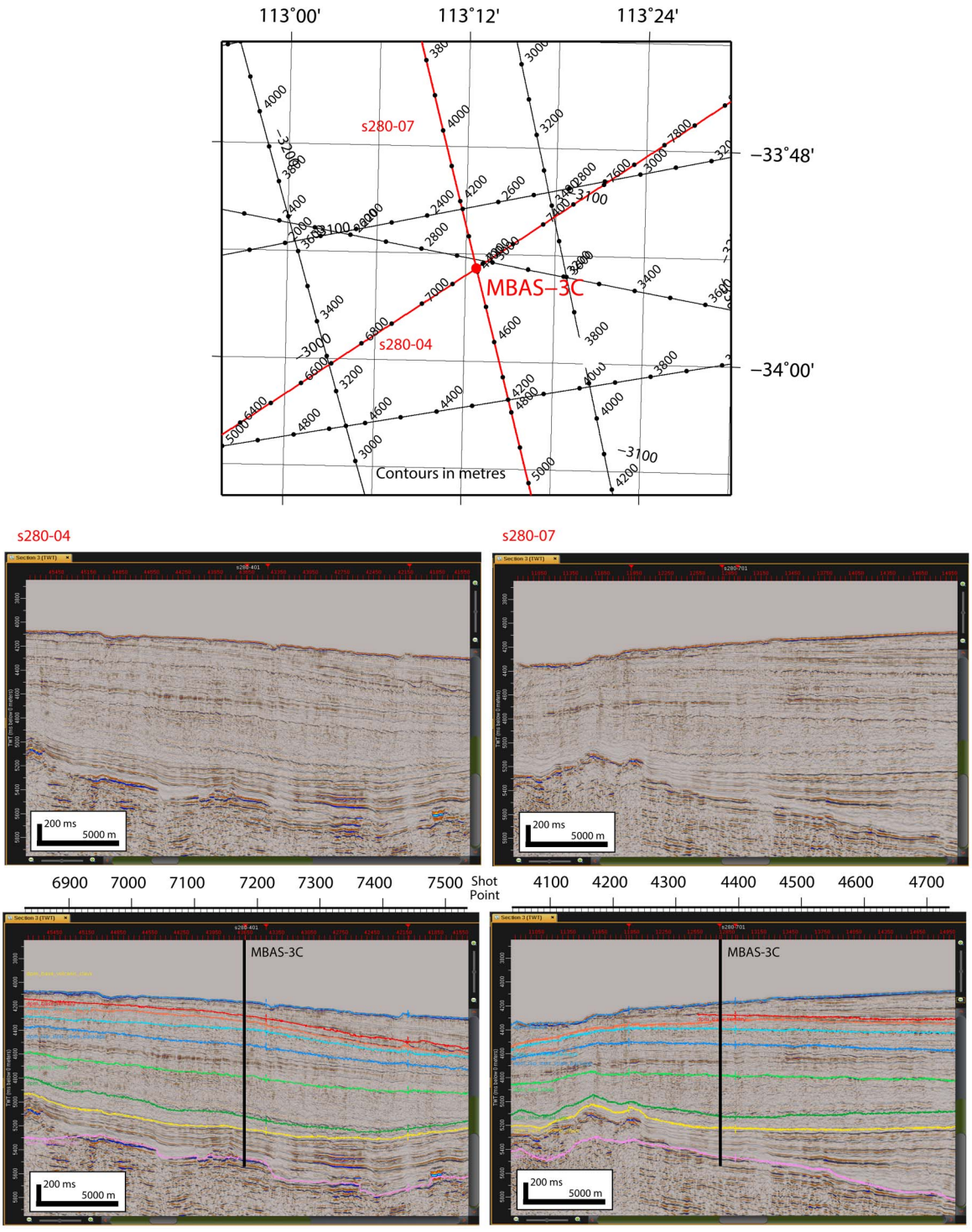

Key Interpreted Horizons
red - base Paleogene deep-marine chalk (Mentelle 10 & 11)
top Cretaceous coccolith-rich chalk (Mentelle 9)
cyan - base coccolith-rich chalk
top Albian/Aptian shales (Mentelle 7a)
blue/green - intra-shale horizons (Mentelle 7a, 7b & 8)
yellow - base shale
top detrital sandstone/glauconitic clay (Mentell 5b & 6)
purple - top Valanginian basalt (Mentelle 5a)

Figure AF8. Track map and seismic profile, alternate Site MBAS-5B.

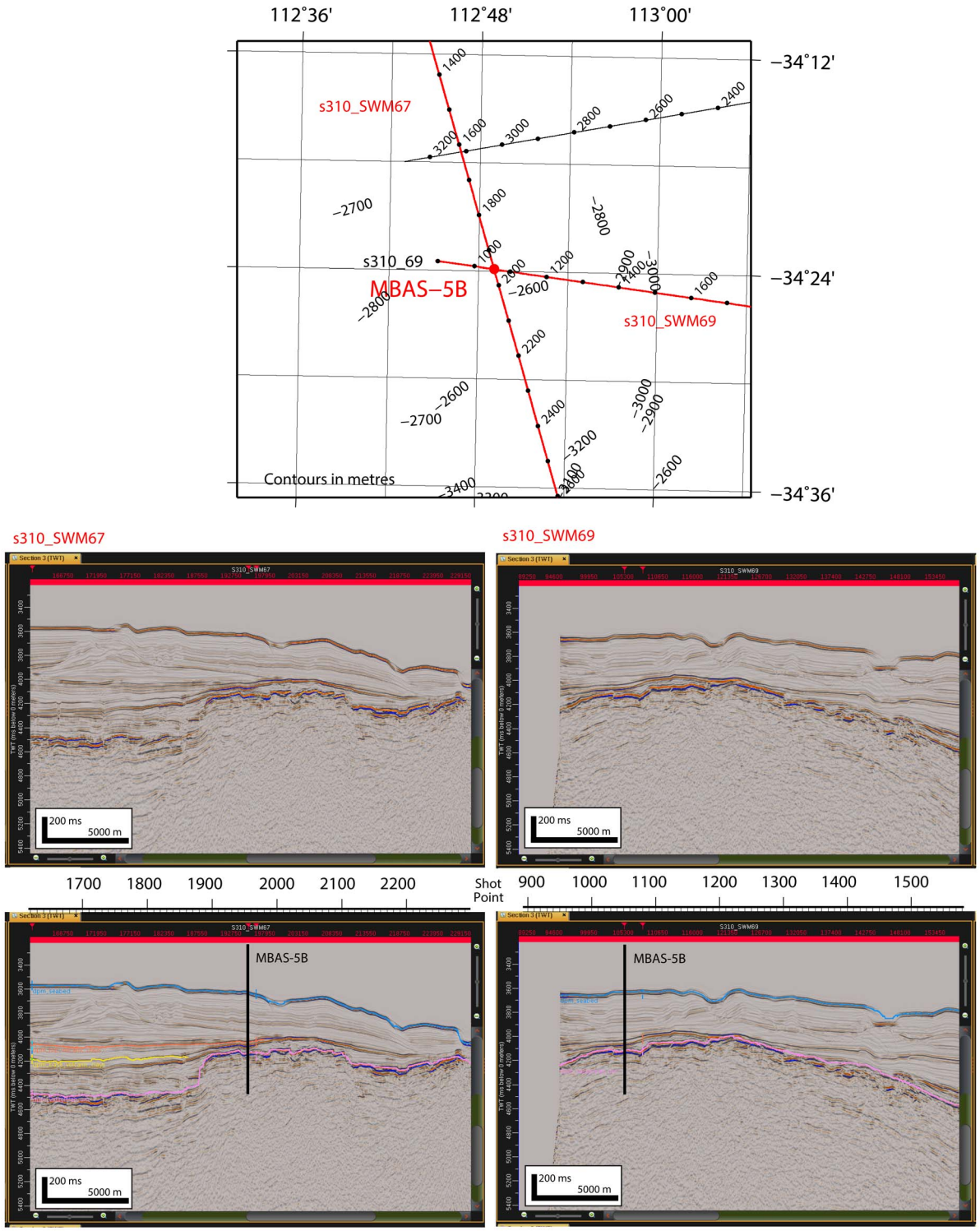

Key Interpreted Horizons
orange - base Paleogene deep-marine chalk and
Cretaceous coccolith-rich chalk (Mentelle 9, 10 & 11Mentelle 9)
top Albian/Aptian shales (Mentelle 7a, 7b & 8)
yellow - base shale
top detrital sandstone/glauconitic clay (Mentell 5b & 6)
purple - top Valanginian basalt (Mentelle 5a)